A reference genome and transcriptome of haustorial development in *Pedicularis groenlandica* reveal diverse trajectories of haustoria-associated gene evolution in parasitic plants

Rachel O. Cohen[1,2]*, Anri Chomentowska[3], Liming Cai[4], and Deren A. R. Eaton[1]*

1. Department of Ecology, Evolution and Environmental Biology, Columbia University, New York, NY 10027 USA
2. Rocky Mountain Biological Laboratory, P.O. Box 519, Crested Butte, CO 81224 USA
3. Department of Evolution, Ecology, and Organismal Biology, Ohio State University, Columbus, OH 43210 USA
4. Department of Biology, University of Florida, Gainesville, FL 32611 USA

* To whom correspondence should be addressed (emails: roc2109@columbia.edu, de2356@columbia.edu)

Summary

- Novel traits frequently evolve by co-opting existing genetic pathways through either the direct repurposing of existing genes or neofunctionatization of duplicated genes. Parasitism represents a major innovation in plants in which a novel organ–the haustorium–evolved to penetrate hosts and extract water and nutrients. Previous studies hypothesized that haustoria-associated genes primarily evolved from root and pollen-associated pathways by neofunctionalization following genome duplications.
- To examine the evolutionary origins of haustoria-associated genes, we generated a chromosome-scale reference genome of the hemiparasite Pedicularis groenlandica (Orobanchaceae) and sampled transcriptomes throughout haustorial development. We identified haustoria-associated genes; examined the expression of these genes and their paralogs across non-haustorial tissues; and investigated overlap in haustoria-associated genes with publicly available haustorial transcriptomes in four additional parasitic plants.
- We identified 5,635 haustoria-associated genes in P. groenlandica. A greater proportion of these genes were associated with pollen tubes (67%) than with roots (33%), evidenced by being either differentially expressed in pollen tubes, nested within pollen tube-associated gene families, or both. Haustoria-associated genes with paralogs that arose after the evolution of parasitism in Orobanchaceae are more likely to be uniquely expressed in haustoria, consistent with neofunctionalization.
- Our results support evidence of both pleiotropy and neofunctionalization as mechanisms by which genetic pathways are co-opted for haustorial function. Haustoria-associated

genes are highly lineage-specific, highlighting a dynamic and ongoing process of independent haustorial co-option of gene functions among parasitic plant lineages.

Key words: genome, haustoria, neofunctionalization, parasitic plants, pleiotropy, pollen tubes, transcriptomics

Introduction

Approximately 1% of flowering plants are parasites on other plants, a strategy that has evolved independently around a dozen times in angiosperms (Westwood *et al.*, 2010). Parasitic plants use a novel organ, the haustorium, to invade host tissues and establish a vascular connection to extract water and/or nutrients. The repeated convergent evolution of haustoria—including their origination from both root (e.g., *Striga*) and stem tissue (e.g., *Cuscuta*) in different lineages— raises fundamental questions about the genomic, developmental, and ecological precursors that enable this transition. Comparative studies have revealed extensive anatomical and physiological convergence in haustoria across a range of lineages (Fernández-Aparicio *et al.*, 2016; Yoshida *et al.*, 2016; Masumoto *et al.*, 2021) and recent genomic studies have identified both lineage-specific and shared molecular pathways associated with haustorial development and function (Westwood *et al.*, 2012; Zhang *et al.*, 2015; Jhu *et al.*, 2021; Kokla *et al.*, 2021; Bawin *et al.*, 2022, 2024). Despite our expanding knowledge of the genes that govern haustorial attachment across parasitic lineages, the evolutionary processes by which genes have been co-opted for haustorial function remain poorly understood.

Parasitic plants span a continuum of host dependence based on developmental requirements (facultative versus obligate parasites), and trophic capacity (hemiparasites, which retain photosynthetic capacity, versus holoparasites, which are fully heterotrophic). Facultative hemiparasites produce lateral haustoria that connect primarily to host xylem, whereas obligate parasites form a terminal haustorium that connects to both xylem and phloem (Press & Graves, 1995; Yoshida *et al.*, 2016). It has been hypothesized that parasitism evolves in a stepwise fashion, with facultative hemiparasitism representing an initial stage that in some lineages gave rise to obligate hemiparasites, and, ultimately, holoparasites (Westwood et al., 2010; Xu *et al.*, 2022). The family Orobanchaceae uniquely spans this full spectrum (including non-parasitic taxa), and encompasses economically significant weeds such as witchweeds (*Striga*) and broomrapes (*Orobanche*) that cause extensive damage to crops worldwide (Joel *et al.*, 2013; Li *et al.*, 2019). As a result, Orobanchaceae has emerged as a model system for the study of haustorial physiology and the genomic basis of parasitic plant evolution.

Haustoria appear, at least in part, to co-opt genetic pathways active in other tissues. Indeed, plants frequently redeploy existing gene repertoires to acquire novel functions and life-history strategies. For example, the co-option of MADS-box genes for floral organ development (originally functioning in gametophyte-sporophyte transitions; Niklas & Kutschera, 2009) and terpene synthases for specialized volatile production and herbivore defense (originally functioning in basic metabolic processes; Abbas et al., 2017). It has been hypothesized that Orobanchaceae, being root parasites, predominantly co-opt root-associated genetic pathways for haustorial function, in addition to some non-root-associated genetic pathways. Consistent with this view, Yang et al. (2015) found that orthologs of haustoria-associated genes are frequently highly expressed in roots of non-parasitic plant species. Curiously, they additionally found that haustorial orthologs are often differentially expressed in pollen and flowers, a result replicated by Yoshida *et al.* (2019). We hypothesize that the relationship between haustoria- and pollen-associated genes results from shared functions between haustoria and pollen tubes, including signal detection, polarized tip growth, cell-wall remodeling, and traversal of foreign tissues. The discovery of haustoria-associated gene homologs expressed in other tissue types may suggest that neofunctionalization of paralogs gave rise to haustorial function. Alternatively, these genes may participate pleiotropically in haustorial development while still functioning in other tissues through tissue-specific regulation.

Novel genes required for haustorial development have been predominantly hypothesized to arise following whole-genome duplications (WGDs), which resulted in duplicate copies that could be co-opted and neofunctionalized (Vogel *et al.*, 2018; Lyko & Wicke, 2021). Signals of ancient WGDs are indeed detectable in Orobanchaceae (Yang *et al.*, 2015; Xu *et al.*, 2022) and *Cuscuta* (Sun *et al.*, 2018), a distantly-related stem-parasitic lineage. Yang et al. (2015) reported that more than half of gene families containing haustoria-associated genes in three species of Orobanchaceae show evidence of ancestral gene duplications, which they hypothesize to be the result of WGDs. In both Orobanchaceae and *Cuscuta*, the WGDs most plausibly linked to haustorial evolution are shared with non-parasitic relatives. Furthermore, Yang et al. (2015) did not evaluate alternative evolutionary hypotheses in addition to WGDs that could explain how genes are co-opted for haustorial function, like other classes of gene duplications (*i.e.* tandem duplications) or pleiotropy. Although gene duplication is a well-recognized engine of evolutionary novelty (Ohno, 1970), plants tend to experience gene and genome duplications at high rates (Moore & Purugganan, 2005) and these phenomena cannot be linked to parasitic plant evolution specifically. Thus, while some haustorial genes may trace to WGD-derived

neofunctionalization, additional evidence is needed to evaluate diverse evolutionary explanations for the co-option of genes for haustorial function following transitions to parasitism.

Over the past decade, newly developed genetic resources in Orobanchaceae have created the opportunity to investigate gene family evolution and tissue co-expression patterns of haustoria-associated genes within a comparative framework (Westwood *et al.*, 2012; Yang *et al.*, 2015; Xu *et al.*, 2022). Many of these studies (Westwood et al. 2012, Yang et al. 2015, Yoshida et al. 2019) leveraged the same transcriptome datasets from the Parasitic Plant Genome Project (Westwood *et al.*, 2012) and contig-level genome assemblies. Advances in genome and transcriptome sequencing and assembly now allow for more accurate identification of haustoria-associated expression, orthology inference, and reconstruction of gene regulatory modules, all of which will aid our ability to determine the identity and function of haustoria-associated genes and evaluate diverse evolutionary hypotheses for their origins.

In this study, we assembled a new chromosome-scale reference genome and annotation of the facultative hemiparasite *Pedicularis groenlandica* (Orobanchaceae), and generated a transcriptomic time series of haustorial development, representing only the third such haustorial expression dataset for a high-quality chromosome-scale genome. Using these data we: (1) identify haustoria-associated genes in *P. groenlandica* and evaluate their chromosomal distribution and overlap in expression with other tissue types; (2) infer co-expression modules and their tissue overlap, and predict regulatory motifs associated with haustorial expression; (3) test the role of neofunctionalization in haustoria-associated gene evolution by comparing tissue-specific expression between paralogs that diverged before versus after the evolution of parasitism in Orobanchaceae; and (4) identify orthology among haustoria-associated genes in *P. groenlandica* and other parasitic plant lineages.

Materials and Methods

Study system – *Pedicularis groenlandica* (Elephant's head lousewort) is an iconic flowering plant of western North American alpine meadows. *Pedicularis* are facultative hemiparasites that attach to a range of host plants through lateral haustoria, most often parasitizing sedges, grasses, and legumes (Piehl, 1963; Ren *et al.*, 2010; DiGiovanni *et al.*, 2017). *Pedicularis* is well-studied for its distinctive pollination biology (Macior, 1968; Grant, 1994; Eaton *et al.*, 2012; Tong & Huang, 2016; Cohen *et al.*, 2025), but little attention has been paid to parasitism within the genus. Two chromosome-scale *Pedicularis* genome assemblies have been published: *P.*

cranolopha (Xu *et al.* 2022) and *P. kansuensis* (Fang *et al.*, 2024). Both studies considered how parasitism has impacted *Pedicularis* genome evolution, including investigations of gene loss, transposable elements, and horizontal gene transfer, but neither examined haustorial gene expression.

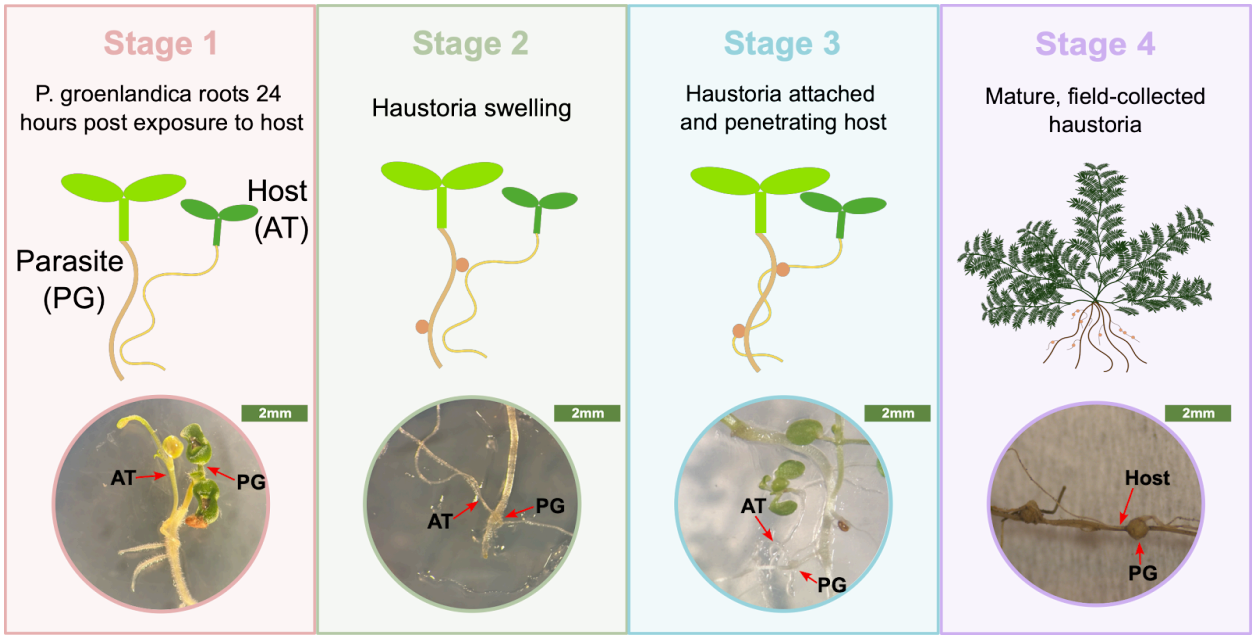

Fig. 1. Stages of haustorial development and attachment sampled in an assay involving the facultative hemiparasite *Pedicularis groenlandica* (PG). Stages 1-3 were sampled from haustoria attachment assays conducted in petri dishes, using *Arabidopsis thaliana* (AT) as a host plant. For stage 4, we sampled mature haustoria in the field, where *P. groenlandica* was attached to a natural *Medicago* host (labeled "Host"). Sampling stages were selected following Westwood et al. (2012).

Tissue collection and genome sequencing – Plant tissues for genome sequencing of *P. groenlandica* were collected at Rocky Mountain Biological Laboratory in Gothic, Colorado, USA in the summer of 2024. Flow cytometry was performed on fresh leaf tissue to estimate genome size, and 5.0g of leaf tissue was sent to Cold Spring Harbor Laboratory (Cold Spring Harbor, NY, USA) for high-molecular weight DNA extraction, PacBio Hifi library preparation and sequencing on a PacBio Revio, and HiC library preparation and sequencing on an Illumina NextSeq2000 to generate 2 x 150bp reads.

For genome annotation and differential expression studies, we collected three biological replicates of young leaf, stem, flower bud, pollen tube, root, and mature haustoria tissues into RNAlater (Invitrogen), which was stored at -80ºC until extraction. To sample pollen tubes, we

germinated fresh *P. groenlandica* pollen on pollen tube growth media, using the methodology employed in Cohen *et al.* (2025). After 24 hours, germinated pollen tubes were flash frozen over a dry ice-ethanol slurry and stored at -80ºC until extraction. RNA was extracted from all tissues using the Qiagen RNeasy Plant Minikit, and Illumina libraries were prepared and sequenced via Illumina MiSeq at Admera Health LLC (South Plainsfield, NJ, USA) to generate 2 x 150bp reads.

Genome Assembly and Annotation – PacBio Hifi reads were filtered to retain only sequences >10kb in length, and assembled into a phased contig-level assembly using Hifiasm v0.19.8 run in "HiC mode" (Cheng *et al.*, 2021). The primary contig-level assembly was analyzed with the Arima Genomics Mapping Pipeline v.03 using YAHS for scaffolding (Zhou *et al.*, 2023), juicer (Durand *et al.*, 2016) to convert the scaffolded assembly into a Hi-C contact map, and JuiceBox Assembly Tools (JBAT; Durand *et al.*, 2016) for manual curation. We evaluated the completeness of our genome with BUSCO v.5.7.0 against eudicots_odb10.1 (Seppey *et al.*, 2019), then soft-masked the genome using RepeatModeler v2.0.6 (Flynn *et al.*, 2020) followed by RepeatMasker v4.1.7p1 (Smit, Hubley & Green 2013–2015).

We structurally annotated the genome using BRAKER3 v3.0.8 with both RNAseq and protein evidence (Stanke *et al.*, 2006, 2008; Quinlan, 2014; Kovaka *et al.*, 2019; Pertea & Pertea, 2020; Brůna *et al.*, 2024; Gabriel *et al.*, 2024). We used RNAseq from all tissues and protein evidence from the Viridiplantae dataset in ORTHODB v.10 (Zdobnov *et al.*, 2021), which were trimmed of adapters and low-quality bases (<Q30) using TrimGalore v0.6.10 (Krueger, 2015), and quality assessed using FastQC v0.12.1 (Andrews, 2010). The annotation completeness was evaluated with BUSCO v.5.7.0 against the eudicots_odb10.1 dataset in transcriptome mode. We functionally annotated the genome using InterProScan with the –goterms tag, and identified the closest *Arabidopsis thaliana* ortholog of each gene with BLAST v2.16.0 (Ye *et al.*, 2006). We conducted a synteny analysis in order to compare *P. groenlandica* to *P. cranolopha* and *O. cumana* (Xu *et al.*, 2022) using MCScan (JCVItools; Tang *et al.*, 2024).

Haustorial time series tissue sampling and sequencing – To generate a time series of gene expression during haustorial growth and development we sampled RNA from *P. groenlandica* haustoria grown in petri dishes while interacting with a host plant. Seeds for this assay were collected from mature seed pods of *P. groenlandica* in the same population as the genome plant, removed from their pods, cleaned of excess tissue, and stored in dry envelopes at 4ºC.

194 *Pedicularis groenlandica* do not require hosts for germination and early growth. We germinated
195 parasites and hosts separately, following the protocol of Westwood et al. (2012) for staged
196 haustorial tissue collection.

197 To promote germination, seeds of *P. groenlandica* were treated with a 200ppM solution
198 of gibberellic acid for 15 minutes, and then sterilized in a solution of 30% bleach, 10% ethanol,
199 60% sterile de-ionized water, and 1 drop of triton, by submerging seeds in the sterilizing solution
200 with agitation for 5 minutes, followed by three washes of shaking in sterile water for three
201 minutes each, and then dried completely. We germinated seeds on plates with 10%
202 Murashige-Skoog (MS) media solution prepared in an autoclave. Seeds were placed ~2cm
203 apart on each plate, and plates were wrapped in Parafilm and placed in a growth chamber on a
204 diurnal cycle with 18 hours of light at 22ºC and 6 hours of dark at 18ºC.

205 *Arabidopsis thaliana* was chosen as the host plant in our haustorial assays due to its fast
206 growth rate and because it has served as a successful host in previous *Pedicularis* haustorial
207 assays (Kee Jia Yee, *personal communication*). Seeds of *A. thaliana* accession
208 Col-0/Rédei-L209478*A* were purchased from Lehle seeds (Round Rock, Texas). Due to their
209 faster rate of germination, we began germinating *A. thaliana* seeds three days after *P.*
210 *groenlandica* germination, in separate plates, following the same germination protocol. Seeds
211 were monitored for germination over a 10 day period, and only those with both cotyledons open
212 and primary root growth >2cm were selected for assays. To initiate the assay, seedlings of *P.*
213 *groenlandica* and *A. thaliana* were carefully removed using sterilized forceps and placed
214 together on a single, sterile, 10% MS plate. We used nutrient-free media at this stage to
215 promote haustorial development. We initially implemented trials in which the *A. thaliana* root
216 was wrapped around the *P. groenlandica* root, but found that placing it ~2mm away from *P.*
217 *groenlandica* promoted greater root and lateral haustorial growth towards *A. thaliana*, and so we
218 proceeded to conduct all trials using this methodology.

219 Our assay included tissue sampled for RNA extraction at four distinct stages (1-4) to
220 establish a time series of haustorial development and attachment (**Fig. 1**). We additionally
221 sampled 1 cm of root tissue from *P. groenlandica* prior to host exposure (stage 0). In the first
222 treatment step (stage 1), we sampled 1 cm of root tissue 24 hours after exposure to the host
223 plant. At the second treatment step (stage 2), bulbous “swelling” haustoria were observed,
224 which form prior to host penetration and attachment. We sampled haustoria, including
225 approximately 1mm of root tissue on each side of the haustorium. In the final treatment step
226 (stage 3), haustoria have fully penetrated and attached to the host. We confirmed this by pulling
227 lightly on the *A. thaliana* root, if the *P. groenlandica* root moved with it we considered the

228 haustoria fully attached. The haustoria were again sampled including 1mm of *P. groenlandica*
229 root tissue above and below. Finally, our assay also included mature, field-collected haustoria
230 (stage 4) sampled from plants dug up during tissue collection for genome annotation. All tissues
231 were collected in triplicate, immediately flash-frozen in liquid nitrogen and stored at -80ºC until
232 extraction. RNA was extracted using the Qiagen RNeasy Plant Minikit, and libraries were
233 prepared using Poly-A selection and sequenced via Illumina MiSeq at Admera Health LLC
234 (South Plainsfield, NJ, USA) to generate 2 x 150bp reads.
235
236 **Differential expression analysis and gene network coexpression analysis in haustorial**
237 **tissues–** As described for the annotation RNA sequences, RNAseq reads were trimmed of
238 adapters and low-quality bases (<Q30) using TrimGalore v0.6.10 (Krueger, 2015), with quality
239 further assessed by FastQC v0.12.1 (Andrews, 2010). All filtered reads, including from leaf,
240 stem, root, flower bud, and pollen tubes, were mapped to the final *P. groenlandica* genome
241 using STAR v2.7.11b (Dobin *et al.*, 2013). Read counts were obtained individually for each
242 replicate at each stage of the haustorial assay (0-4), as well as for each non-parasitic tissue.
243 Following alignment, we used featureCounts (Liao *et al.*, 2014) to count reads mapped to each
244 annotated gene.
245 To identify differentially expressed genes, we analyzed expression counts in the R
246 package DESeq2 v1.42.1 (Love *et al.*, 2014). We compared haustorial growth stages (Stages
247 1-4) against non-parasitic tissue-types (leaf, stem, root, flower bud, pollen tubes and Stage 0) to
248 identify genes that were either up- or down-regulated in each haustoria time stage compared to
249 non-parasitic tissue. Prior to running DESeq2, we excluded low count genes (counts <10). To
250 visually confirm the expected similarity among replicates within tissues, and between more
251 similar tissues, we performed a principal components analysis of the gene expression data from
252 DESeq2. A gene was determined to be differentially expressed in haustoria if it had a
253 log2FoldChange>2 (up-regulated) or <–2 (down-regulated) relative to non-parasitic tissues, and
254 an adjusted p-value <0.05. We compiled a list of “haustoria-associated” genes, which includes
255 the set of genes that were differentially expressed in at least one stage (1-4) of the haustorial
256 assay. We assessed the distribution of haustoria-associated genes across the *P. groenlandica*
257 genome and calculated the correlation between haustoria-associated gene density and overall
258 gene density using Pearson’s correlation coefficient and a Student’s T-test.
259 To identify modules of co-expressed genes, we implemented weighted gene
260 co-expression network analysis (WGCNA). Following the methodology of Gilman *et al.* (2022),
261 we input the quantified transcripts per million (TPM) for each gene to WGCNA v1.73 in R

262 (Langfelder & Horvath, 2008). We assessed which of the resultant co-expression gene modules
263 were correlated with gene expression in each of the tissues included in analyses (haustoria,
264 leaf, stem, root, flower bud, pollen tubes) by calculating the Pearson's correlation coefficient and
265 assessing significance by a student's asymptotic t-test. A module was designated as
266 haustoria-associated if its expression was significantly correlated with haustorial samples
267 (stages 1-4) compared to non-haustorial samples (stage 0 and other tissues). To determine
268 functional descriptions of the genes in each module, we first identified their orthologs in *A.*
269 *thaliana* through BLAST against the TAIR *A. thaliana* Genome V (Lamesch *et al.*, 2012), then
270 determined the Gene Ontology biological process terms that were enriched in each module
271 using the "enrichGO" function in the *clusterProfiler* in R (v4.10.1; Wu *et al.*, 2021).
272
273 **Overlap of differentially expressed genes and regulatory motifs in haustoria and**
274 **non-parasitic tissues –** To investigate the hypothesis that haustoria-associated genes may
275 also be differentially expressed in other tissues, we measured the overlap in genes that were
276 differentially expressed in both haustoria and leaf, stem, root, flower bud, pollen tubes.
277 Differential expression analysis requires a pairwise comparison (*i.e.* genes are up-regulated in
278 haustoria *compared* to pollen tubes). We independently quantified differential expression in
279 each individual overlap analysis, making sure haustoria and the focal tissue were always
280 compared to the same 'control' set. For example, when investigating haustoria- and pollen
281 tube-associated gene overlap, we identified genes differentially expressed in haustoria
282 compared to leaf, stem, root, and flower bud, and genes differentially expressed in pollen tubes
283 compared to the same set of tissues. We proceeded in this manner, systematically comparing
284 haustoria and the focal tissue to the identical control sets, then assessed how many of the
285 genes overlapped among haustoria and the focal tissue. Through this analysis, we identified not
286 only the overlap in differential expression of haustoria-associated genes with other tissues, but
287 also identified a set of "haustoria-specific" genes that are only differentially expressed in
288 haustoria.
289 We additionally investigated whether co-expressed networks of haustorial-associated
290 genes shared enriched regulatory motifs with other tissue-associated modules. To identify
291 enriched motifs associated with each tissue, we first identified WGCNA modules of genes
292 whose expression patterns were correlated with each tissue, using Pearson's correlation
293 coefficient, as above. Because WGCNA modules contain genes that are not tissue-associated
294 as determined by the differential expression analysis, we searched for enriched motifs within
295 2kb of only tissue-associated genes in each tissue-associated module using XSTREME (Meme

296 v5.5.8; Bailey *et al.*, 2009) following methods in Chomentowska *et al.* (2025). We identified
297 enriched motifs that overlapped in haustoria and other tissues in both sequence and locus.
298 Similar to our approach for identifying overlap in differentially expressed genes among haustoria
299 and non-parasitic tissues, for each individual motif overlap analysis, we independently identified
300 coexpression modules with WGCNA and evaluated module correlation with each focal tissue
301 excluding haustoria, then haustoria modules excluding the focal tissue such that the haustoria
302 and focal tissue were again compared to an identical group of "control" tissues when
303 determining module-tissue correlation.
304 Because pollen tubes and haustoria had the highest overlap in terms of
305 tissue-associated genes and regulatory motifs, they were further evaluated. For the set of genes
306 that overlapped between haustoria and pollen tubes we assigned molecular function GO terms
307 by identifying their orthologs in *A. thaliana*, then using the "enrichGO" function in the R package
308 *clusterProfiler* (v4.10.1; Wu et al., 2021). Using the modules constructed during overlap
309 analyses, we asked if haustoria- and pollen tube-associated genes were similarly grouped into
310 co-expression modules more often than expected by chance. To do this, we constructed a
311 contingency matrix which included the 'observed values' of overlapping haustoria- and pollen
312 tube-associated genes assigned to haustoria- and pollen tube-associated modules, respectively.
313 To set null expectations, we performed a permutation-based test in which we randomly shuffled
314 module assignments while preserving the number of genes in each module. We conducted
315 2,000 permutations and recalculated the overlap contingency table with these 'expected values',
316 then recorded the number of times observed values were greater than or equal to expected
317 values and calculated empirical *p*-values. To account for multiple testing across all module pairs,
318 *p*-values were adjusted using Benjamini–Hochberg false discovery rate (FDR). Finally, we
319 functionally annotated the shared enriched motifs by identifying the family of transcription
320 factors with which each motif interacts using TOMTOM (Meme v5.5.8; Bailey et al., 2009),
321 comparing our enriched motifs against known motif annotations in the JASPAR database
322 (Rauluseviciute *et al.*, 2024).
323
324 **Analysis of haustorial gene trees and gene duplications –** To evaluate the hypothesis that
325 haustoria-associated genes evolved by neofunctionalization following gene or genome
326 duplication events in a non-parasitic ancestor of Orobanchaceae, we examined the phylogenetic
327 relationships of haustoria-associated genes with respect to their paralogs and orthologs, and
328 their differences in tissue-specific expression. We downloaded protein sequences of four
329 publicly available non-parasitic genomes from NCBI Genbank and JGI Phytozome: *Mimulus*

330 *guttatus* (NONTOL v4.0, DOE-JGI), *Salvia miltiorrhiza* (GCF_028751815.1; Pan *et al.*, 2023),
331 *Solanum lycopersicum* (ITAG5.0; Zhou *et al.*, 2022), and *Arabidopsis thaliana* (TAIR10;
332 Lamesch *et al.*, 2012), and assembled orthogroups using Orthofinder v3.0.8 (Emms & Kelly,
333 2019) run with default settings. Orthogroups were filtered to retain only those that contained one
334 or more haustoria-associated genes. Multiple sequence alignments from Orthofinder were
335 cleaned and trimmed using a custom Python script, and gene trees were inferred by RAXML-ng
336 v1.2.2 (Kozlov *et al.*, 2019) with support assessed from 100 non-parametric bootstraps. Many
337 trees contain multiple gene copies per species, so we used the Duplication-Transfer-Loss model
338 in GeneRax v2.1.3 (Morel *et al.*, 2020) to obtain reconciled and rooted genes trees based on the
339 species tree topology, retaining trees with >3 genes (*i.e.* tips), according to default GeneRax
340 settings.
341 For each *P. groenlandica* haustoria-associated gene in each rooted orthogroup tree, we
342 identified paralogs and recorded their tissue-specific expression. Tree-based operations were
343 performed in the Python package toytree v.3.0.10 (Eaton, 2020) to identify: the closest
344 non-haustoria-associated paralog that is more closely related than the closest ortholog (i.e., it
345 arose by duplication within Orobanchaceae); and the closest non-haustoria-associated paralog
346 that is equal to or more distantly related than the closest ortholog (*i.e.*, it arose by duplication in
347 an ancestor of Orobanchaceae; *see* ***Fig. 5a***). If multiple paralogs were equally related to the
348 haustoria-associated gene, one was chosen at random. For each gene, we recorded the tissue
349 in which it was differentially expressed, as measured above.
350 To validate our approach, we visually examined many gene trees, including for several
351 selected genes with known haustorial function. We searched TAIR10 (Lamesch et al., 2012) to
352 identify the *A. thaliana* gene locus identifiers for homologs of genes that have been
353 experimentally shown to affect haustoria development and hormone signaling or pollen tube
354 growth and signaling. This includes ROOT MERISTEM GROWTH FACTOR (RGF), which
355 (Fishman *et al.*, 2025)demonstrated is necessary for haustorial development in the hemiparasite
356 *Phtheirospermum japonicum*; KARRAKIN INSENSITIVE-2 (KAI2), which has been shown to
357 have paralogs that enable ultra-sensitive strigalactone receptors in Orobanchaceae (Wang *et*
358 *al.*, 2021; Takei *et al.*, 2024), two deep homologs of KAI2, DWARF14 (D14), and
359 DWARF14-LIKE2 (DLK2), and pollen tube growth and guidance genes Cyclic Nucleotide-Gated
360 Channel 18 (CNGC18; von Besser et al., 2006), HAPLESS 2 (HAP2; Daher & Geitmann,
361 2012), and Actin-Depolymerizing Factor 7 (ADF7; Gao *et al.*, 2016).
362

363 **Modeling the effect of gene duplications –** To quantify the relative importance of gene
364 duplications to the evolution of haustorial specificity in gene expression, we compared the
365 number of genes that are haustoria-specific (*i.e.*, only differentially expressed in haustoria) to
366 those that are differentially expressed in multiple tissues including haustoria, and whether
367 haustoria-specific expression is predicted by the orthogroup having recent and/or ancient
368 duplications. For each haustoria-associated gene, we recorded whether it was
369 haustoria-specific, whether a recent paralog exists in the gene tree, and whether an ancient
370 paralog exists. The number of *P. groenlandica* genes in each orthogroup was included as a
371 covariate (log transformed and centered before fitting). We fit a population-averaged logistic
372 model using generalized estimating equations (GEE; Binomial, logit link) with genes clustered
373 by orthogroup, an exchangeable working correlation, and robust (sandwich) standard errors.
374 Models were fit using statsmodels (Seabold & Perktold, 2010) in Python. Two-sided Wald tests
375 were used to assess coefficients, with odds ratios and 95% confidence intervals. We compared
376 the effect of recent versus ancient paralogs via a Wald X^2 test, and computed average marginal
377 effects.
378
379 **Orthology and expression overlap of haustoria-associated genes among parasitic plant**
380 **species –** To investigate the extent to which haustoria-associated genes in *P. groenlandica* are
381 shared with other parasitic plant lineages, we examined differential expression and orthology
382 with other haustoria development datasets. We restricted our analyses to four datasets with
383 transcriptomic time-series of haustorial development analogous to our dataset (*i.e.*, RNA
384 sampled from at least stages 1-3). This included: *Cuscuta campestris* (Bawin *et al.*, 2024),
385 *Phtheirospermum japonicum* (Kokla *et al.*, 2021), *Striga hermonthica* (Westwood *et al.*, 2012),
386 and *Orobanche aegyptiaca* (Westwood *et al.*, 2012). The quality of these datasets varied—*S.*
387 *hermonthica* and *O. aegyptiaca* were generated in 2012, whereas *C. campestris* and *P.*
388 *japonicum* were generated using more modern technologies since 2020. We utilized the control
389 haustorial dataset from Kokla et al. (2022) whose main research focus was repression of
390 haustorial formation by nitrogen, rather than the process of haustorial formation itself.
391 In order to identify haustoria-associated genes by stage in each of these datasets, we
392 followed the same pipeline that was used in *P. groenlandica*. A publicly available reference
393 genome is available for each species with the exception of *O. aegyptiaca*. For this taxon, we
394 instead mapped reads to the *O. cumana var. cumana* genome (Xu et al., 2022). Because reads
395 mapped at a sufficiently high rate (average 66.8% mapping rate across all tissues and stages),
396 we proceeded with the remainder of the pipeline. Genes from *P. groenlandica* and the four

397 published genomes were classified into orthogroups using Orthofinder v3.0.8 (Emms & Kelly,
398 2019). We quantified orthogroup overlap among species' haustoria-associated genes, then
399 functionally annotated the haustorial orthologs by identifying their *A. thaliana* orthologs, followed
400 by conducting a Gene Ontology term enrichment analysis using *clusterProfiler*, as described
401 above.
402

403 Results

404 **The *P. groenlandica* genome –** The *P. groenlandica* genome represents a new, high-quality
405 genomic resource in *Pedicularis* and Orobanchaceae. The assembled haploid genome size is
406 1.38Gb, consistent with the flow cytometry estimate (C=1.59; **Fig. S1**). We scaffolded the
407 genome into eight highly contiguous chromosomes which include 91.6% of nucleotide base
408 pairs (**Fig. 2**). The BUSCO completeness score was 96.5% (Single-copy: 90.5%, Duplicates:
409 6.1%). The *P. groenlandica* genome contained a high proportion of repetitive elements, with
410 repeats making up 76.48% of the genome. A large proportion of repeats (44.14%) are long
411 terminal repeats (LTRs). Our genome has high synteny to *P. cranolopha* (Xu *et al.*, 2022), but
412 exhibit rampant rearrangement with respect to *Orobanche cumana var. Cumana*. We annotated
413 27,006 unique protein coding genes. The BUSCO score of the annotation was 94.3%
414 (Single-copy: 59.6%, Duplicates: 34.7%).
415

416 **Haustoria-associated gene expression, function, and regulation –** Across our RNAseq
417 libraries, we obtained an average of 27.84 million reads per replicate per tissue, of which an
418 median of 20.89 million reads (83.01%) uniquely mapped to the *P. groenlandica* genome. All
419 protein coding genes were represented in the final count dataset. Differential expression
420 analysis in DESeq2 identified 5,635 haustoria-associated genes across all four stages (**Fig.
421 3a-b**). The density of haustoria-associated genes across chromosomes was highly correlated
422 with the density of all genes (P<0.001; **Fig. 3d**).
423 In stage 1, twenty-four hours after host exposure, 3,734 genes were differentially
424 expressed, and showed enrichment for biological process GO terms relating to mitotic cell
425 division, DNA replication, and cell wall biogenesis. In stage 2, when haustoria began to swell,
426 2,054 differentially expressed genes showed functions enriched in pigment biosynthesis,
427 tetrapyrrole metabolism, ion transport, and unidimensional cell growth. In stage 3, during host
428 invasion, 679 genes were differentially expressed, which were enriched for pollen tube growth,
429 pollination, cellular tip growth, and unidimensional cell growth. In mature haustoria (stage 4),
430

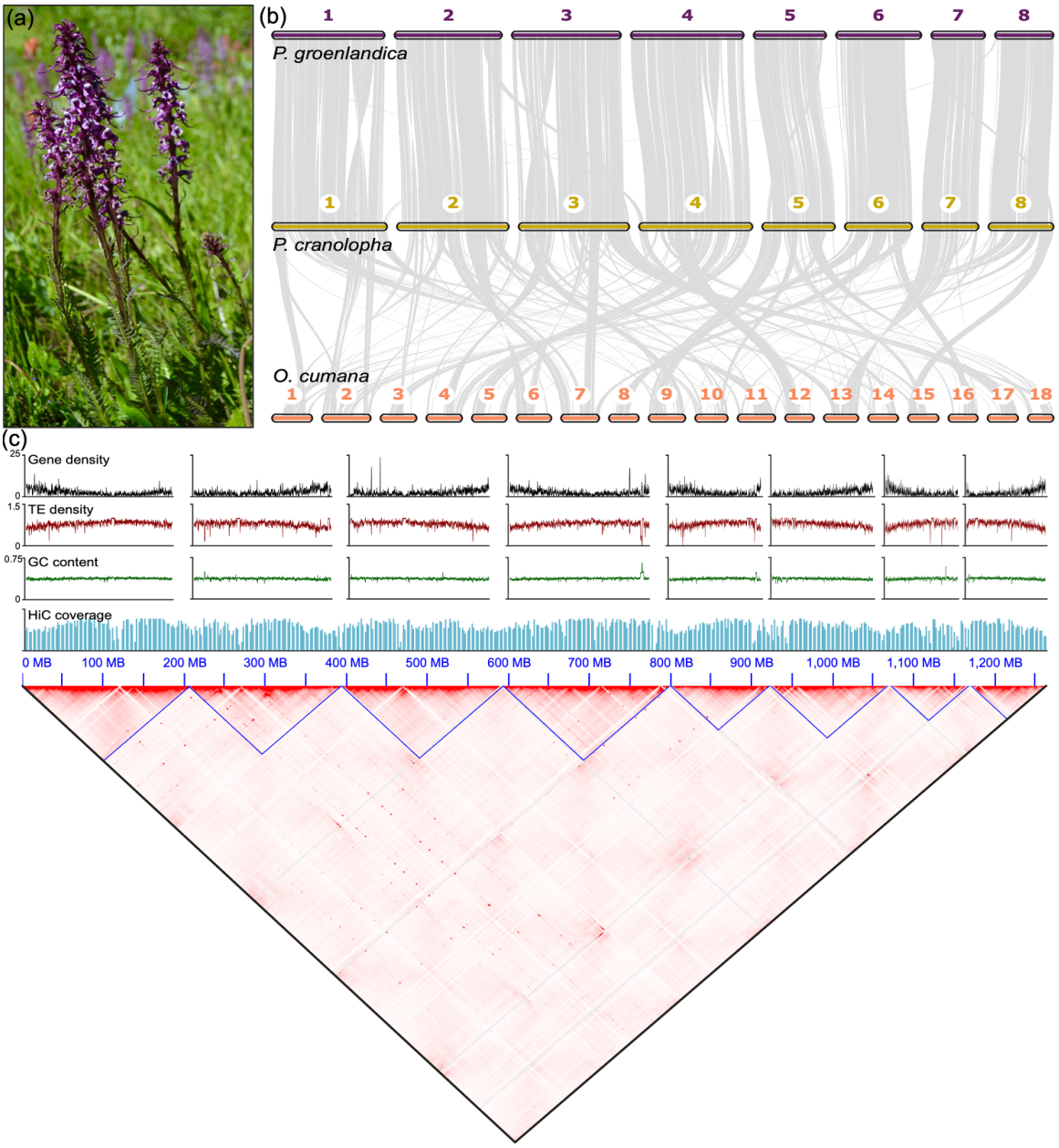

Fig. 2. Chromosome-scale assembly of the *Pedicularis groenlandica* genome. **a)** Photo of *P. groenlandica* (Elephant's head lousewort). **b)** Gene synteny between the eight chromosomes of *P. groenlandica* and *P. cranolopha*. Both *Pedicularis* species have highly rearranged genomes with respect to the *Orobanche cumana var. cumana* genome (Xu *et al.*, 2022). **c)** Gene density, transposable element (TE) density, GC content, and HiC sequence coverage statistics along 10kb sliding windows in the *P. groenlandica* genome. Genes and TE's are distributed evenly across the genome, and there are few peaks in GC content. We show the HiC contact-map shows 8 contiguous chromosomes in *P. groenlandica*.during correlation tests. 2,047 genes were differentially expressed, showing enrichment for light response and photosynthesis biological process GO terms.

443 2,047 genes were differentially expressed, showing enrichment for light response and
444 photosynthesis.

445 Of the 32 co-expression network modules identified by WGCNA, we identified ten that
446 are significantly correlated (P < 0.05) with haustoria, and assigned functional descriptions to
447 each based on the most enriched GO terms among genes in the module (**Fig. 3c**). These one of
448 the haustoria-associated modules was enriched for pollen tube-associated functions (biological
449 process GO terms like, pollination, unidimensional cell growth, pollen tube development, and
450 pollen tube growth, among others; **Fig. S2**). Conservatively, we focus on the modules identified
451 as significantly associated with haustoria compared to all other tissue-types included in the
452 study (**Fig 3c**).

453

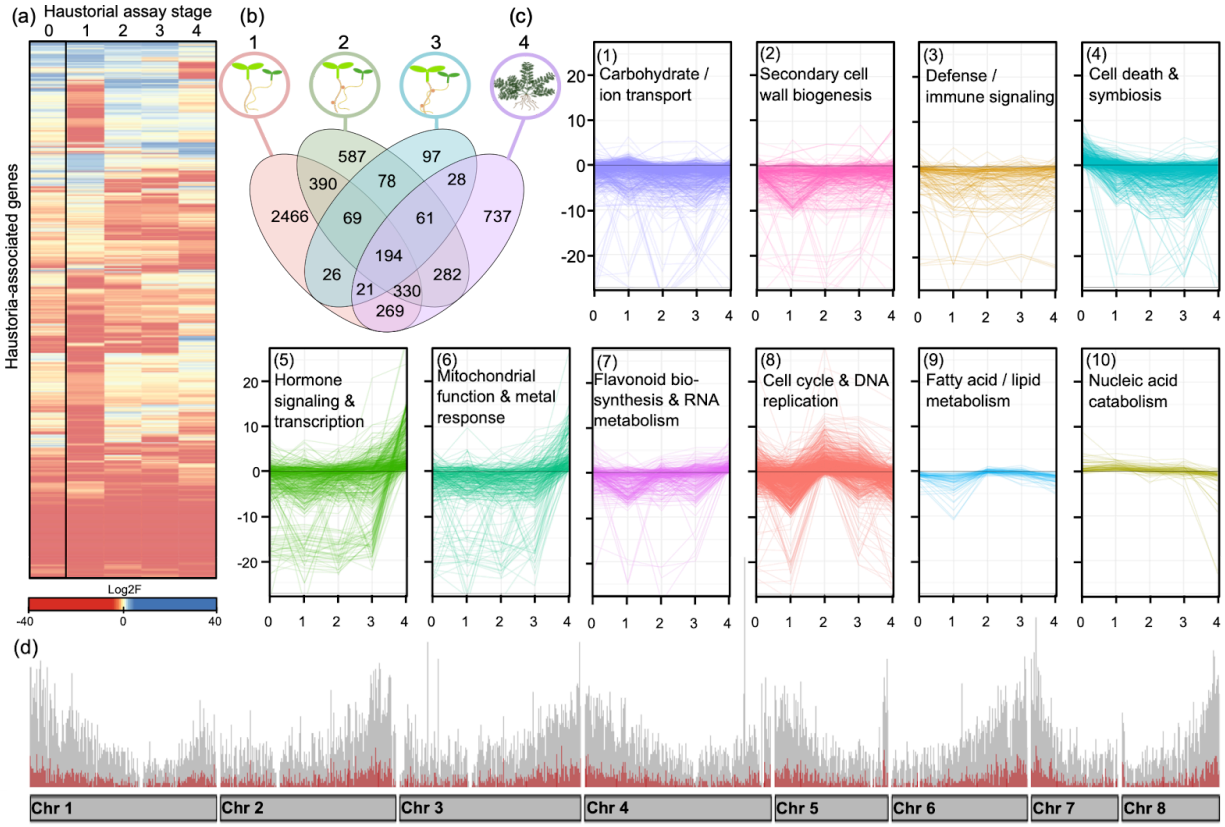

454 **Fig. 3.** Haustoria-associated genes and their gene expression in *Pedicularis groenlandica*. We
455 identified 5,635 haustoria-associated genes, including both up- and down-regulated genes. **a)**
456 Heatmap of Log2FoldChange values for each haustoria-associated gene. Red indicates
457 down-regulation and blue up-regulation. We include "Stage 0", young roots pre-host exposure,
458 to show changes in gene expression across the entirety of haustorial development and
459 attachment. **b)** Venn diagram showing the overlap in genes involved in haustorial response
460 across the four stages. Stage 1, response 24 hours post-host exposure, had the highest number
461 of stage-specific genes. **c)** Changes in gene expression among the sets of genes within 10
462 haustoria-associated WGCNA modules, representing co-expressed molecular responses to

host presence, haustorial initiation, and haustorial attachment. Lines in each module plot show the change in gene expression of a single gene throughout the stages of haustorial development. Each module is labeled according to the most enriched GO biological process terms for the set of genes. **d)** Bar chart depicting haustoria-associated gene density (red) compared to general gene density across the genome (grey), calculated in 10kb sliding windows. The grey bars along the horizontal axis represent *P. groenlandica*'s eight chromosomes.

Haustoria-associated gene and regulatory motif overlap with non-parasitic tissues– Our set of haustoria-associated genes has the highest overlap with genes associated with pollen tubes; more than any other tissue-type, including roots (**Fig. 4a**). Here, gene overlap means that the same loci were identified as differentially expressed in both haustoria and a particular tissue. Similarly, regulatory motifs enriched in the flanking regions of haustoria-associated genes within individual WGCNA co-expression modules correlated with haustorial tissues showed the highest level of overlap with pollen tubes (**Fig. 4b)**, although the degree of overlap was lower when measured by motif identity (**Fig 4a**). Despite sharing a substantial set of genes, haustoria and pollen tubes often exhibit opposite differential expression patterns: genes up-regulated in pollen tubes are frequently down-regulated in haustoria (**Fig. 4b**). This resulted in the expression profiles of haustoria and pollen tubes being the most distinct from one another among all tissues considered (**Fig. S3**). Finally, across all co-expression modules identified as haustoria-associated during haustoria/pollen tube overlap analyses, haustoria- and pollen tube-associated genes were grouped together more often than we would expect due to chance alone (**Fig 4c**, FDR-adjusted $P<0.05$).

Divergence between haustoria-associated genes and their paralogs – The 5,635 haustoria-associated genes identified in *P. groenlandica* were grouped into 3,761 orthogroups, including alternative splice isoforms predicted by BRAKER3. After collapsing isoforms (which grouped into the same orthogroup 99.99% of the time), this dataset contains 4,718 *P. groenlandica* genes, corresponding to a mean +/- stdev of 1.25 +/- 0.73 genes per orthogroup. We identified 2,054 haustoria-associated genes (44%) that have at least one non-haustoria-associated paralog. Of these, 1211 (59%) have a paralog that arose from a duplication after the divergence between Orobanchaceae and *Mimulus*, while 1121 (55%) have a paralog that arose ancestral to this split. Only 278 (14%) of haustoria-associated genes have both types of paralogs in the same gene tree.

We examined the divergence and overlap in tissue-specific expression between paralogs in each category, which, for convenience, we hereafter refer to as paralogs that arose

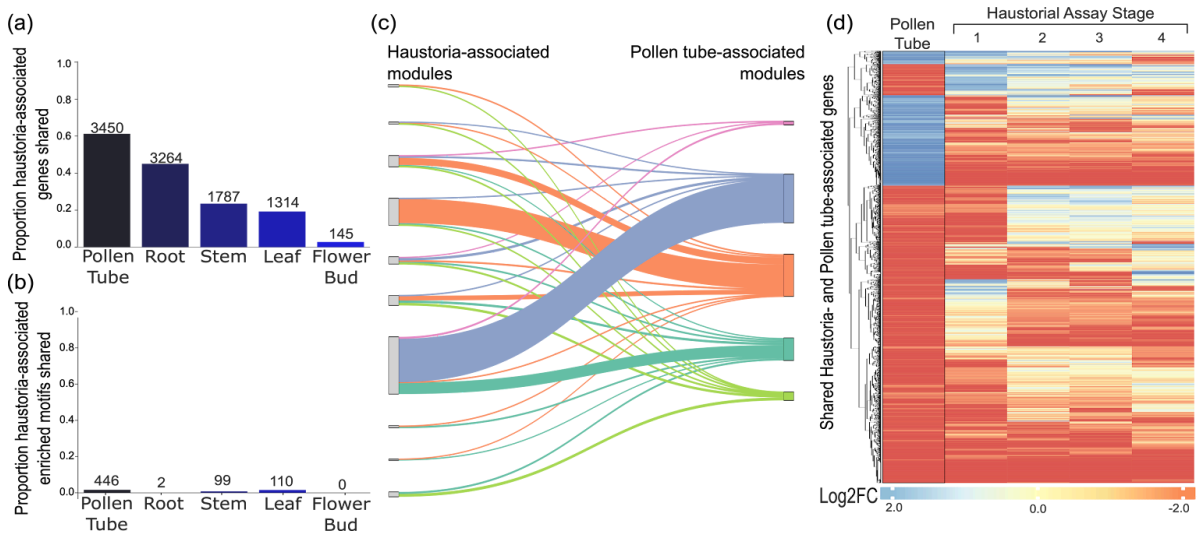

Fig. 4. Overlap of haustoria-associated genes and regulatory motifs with non-parasitic tissues. Bar charts showing **a)** the proportion of haustoria-associated genes and **b)** enriched regulatory motifs that overlap with non-parasitic tissues. We additionally report the count of overlapping genes and motifs above each bar. We show that haustoria-associated genes and motifs overlap most often with pollen tube's. **c)** Relative grouping of genes into co-expression modules in haustoria and pollen tubes. Haustoria- and pollen-associated genes were grouped together in co-expression modules more often than expected due to chance alone (P<0.05 in each haustoria-associated module). **d)** Heatmap of gene expression (Log2FoldChange) of overlapping haustoria- and pollen tube-associated genes. Blue values are up-regulated genes, and red are down-regulated genes. Many shared genes show the opposite direction of expression in pollen tubes versus haustoria.

from "recent" versus "ancient" duplications. For genes that were the product of recent duplications, paralogs of haustoria-associated genes were more frequently differentially expressed in pollen tubes (40%) than any other tissue type (3-13%), and the remaining half (52%) were not differentially expressed in any non-parasitic tissue considered (**Fig. 5a**). For ancient paralogs, an even greater proportion are associated with pollen tubes (57%) and very few in roots (19%; **Fig. 5b**). In addition, paralogs expressed in pollen tubes are often exclusively found in this tissue, while root associated paralogs tend to be expressed in multiple tissue-types (**Fig. 5a-b**).

Selected gene trees – We inspected many gene trees and selected several that demonstrate interesting patterns among genes that contain orthologs with demonstrated function in haustorial development and attachment in other parasitic lineages. We detected haustoria-associated genes in both KAI2 and D14, which are receptors of strigolactones in Orobanchaceae used to detect host plants (Mutuku et al. 2020). A haustoria-associated gene

was also found within the homolog DLK2, which has not been previously implicated in parasitism. In all three groups the haustoria-associated genes were also differentially expressed in pollen tubes, as well as roots in the case of DLK2. Only KAI2 contains a paralog, which was not differentially expressed in haustoria or any other tissues examined.

Two homologs of ROOT GROWTH FACTOR that are associated with haustorial morphogenesis contain both haustoria-associated genes and non-haustoria-associated paralogs in *P. groenlandica* (**Fig. 5g-h**). In RGI4 an ancient duplication separates a haustoria-associated gene that is differentially expressed in several tissues, including during stage 1 of the haustorial assay, from a non-haustoria-associated paralog that is uniquely expressed in pollen tubes. RGFR2 similarly contains an ancient duplication separating a haustoria-specific gene that was differentially expressed during stage 2 of the haustorial assay, from a paralog that is differentially expressed in pollen tubes and roots.

Three orthogroups were selected that contain haustoria-associated genes among homologs of *Arabidopsis* genes with known function in pollen-tube growth and guidance (CNGC18, HAP2, and ADF7; **Fig. 5i-k**). In CNGC18 and ADF7, we observe a haustoria-associated gene separated by a “recent” duplication from a non-haustoria-associated paralog that is differentially expressed in pollen-tubes and other tissues. In HAP2 the *P. groenlandica* ortholog is haustoria-specific. A haustoria-associated gene in all three orthogroups was expressed during stage 1 of the haustorial assay. Overall, this set of tree visualizations (**Fig. 5d-k**) demonstrates the diversity of patterns of gene duplication and expression divergence across gene families containing haustoria-associated genes in *P. groenlandica.*

Modeling the effect of gene duplications – To quantify the relative importance of gene duplications for the evolution of haustoria-specific expression, we compared the number of genes that are haustoria-specific to those that are differentially expressed in multiple tissues, increases the odds that a haustoria-associated gene is haustoria-specific (OR=1.59, 95% CI 1.27–2.00, $p<0.001$). In contrast, ancient non-haustoria-associated paralogs showed no significant association (OR=0.86, 95% CI 0.70–1.05, $p=0.13$). A direct Wald test confirmed the difference between recent and ancient effects ($\chi^2=23.19$, $p=1.5\times10^{-6}$). The average marginal effects from the GEE indicate that recent non-haustoria-associated paralogs increase the probability of haustoria-specific expression by 7.6 percent (SE=1.9, $p<0.001$), whereas ancient paralogs are associated with a non-significant −2.5 percent change (SE=1.7, $p=0.13$).

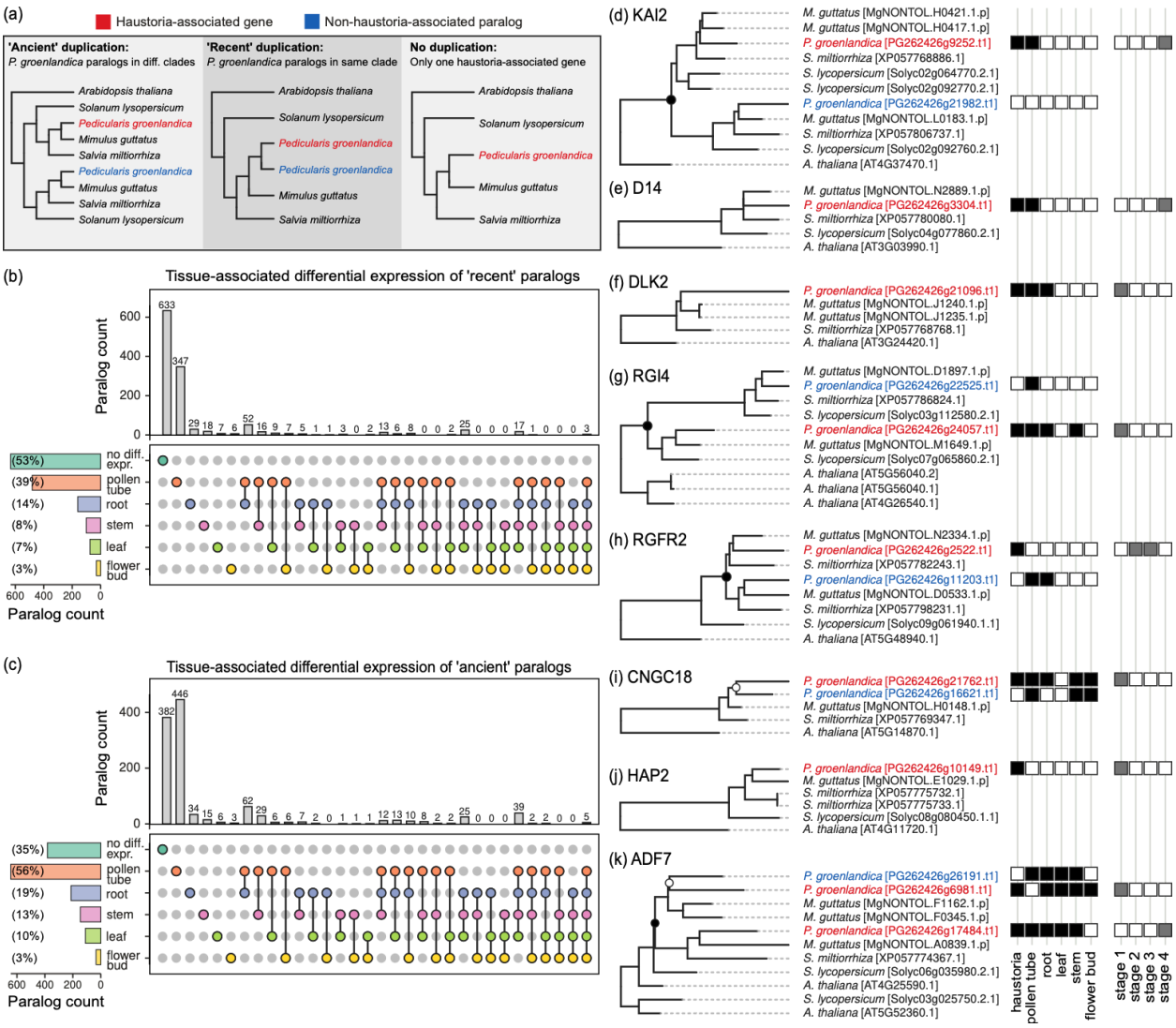

Fig 5. Differential expression of Pedicularis groenlandica haustoria-associated genes and their paralogs across multiple plant tissues. (a) The closest non-haustoria-associated paralog separated by either a "recent" or "ancient" gene duplication was identified in each orthogroup gene tree, if present. (b-c) The expression profiles of non-haustoria-associated paralogs are summarized in upset plots for "recent" (b) and "ancient" (c) paralogs, respectively. Most non-haustoria-associated paralogs of haustoria-associated genes are either not differentially expressed in any tissues, or are differentially expressed in pollen tubes. (d-k) Example orthogroup gene trees showing expression profiles for haustoria-associated genes and their paralogs, if present. These orthogroups contain homologs associated with haustorial development or pollen tube guidance. Open circles indicate "recent" gene duplications, and closed circles "ancient" gene duplications. For haustoria-associated genes we show the haustorial assay stage in which they were differentially expressed.and whether this can be predicted by the presence of recent and/or ancient gene duplications. Using a GEE logistic model, we found that the presence of a recent non-haustorial paralog

Diverging haustorial gene repertoires across parasitic plant lineages – Among the haustorial transcriptome datasets from five parasitic species (4 Orobanchaceae, 1 *Cuscuta*), we

identified a highly variable number of haustorial-associated genes. It was lowest among the two oldest datasets (*S. hermonthica*=120, *O. aegyptiaca*=472). By contrast, a much greater number of haustoria-associated genes was detected in the three recent datasets (*C. campestris*=10,396, *P. japonicum*=1,058, and *P. groenlandica*=5,635). We restricted our main comparative analysis to these three datasets (**Fig. 6a)**. Genes in shared orthogroups were expressed in each of the four stages of haustorial development (**Fig. 6c**). Orthology analysis identified haustoria-associated gene families shared between Orobanchaceae and *Cuscuta*, and an even greater number that are lineage-specific (**Fig. 6b**). Within the five species dataset, we identified only two orthogroups shared among all Orobanchaceae, compared to a majority of species-specific orthogroups (**Fig. S3**). The highest orthogroup overlap was among the three modern datasets, with 660 shared between *P. groenlandica* and *C. campestris*, 258 shared between *P. japonicum* and *P. groenlandica*, and 90 shared between *C. campestris* and *P. japonicum*. Among all five species, the highest number of overlapping orthogroups occurred in those that contained genes which were differentially expressed during haustorial swelling (stage 2).

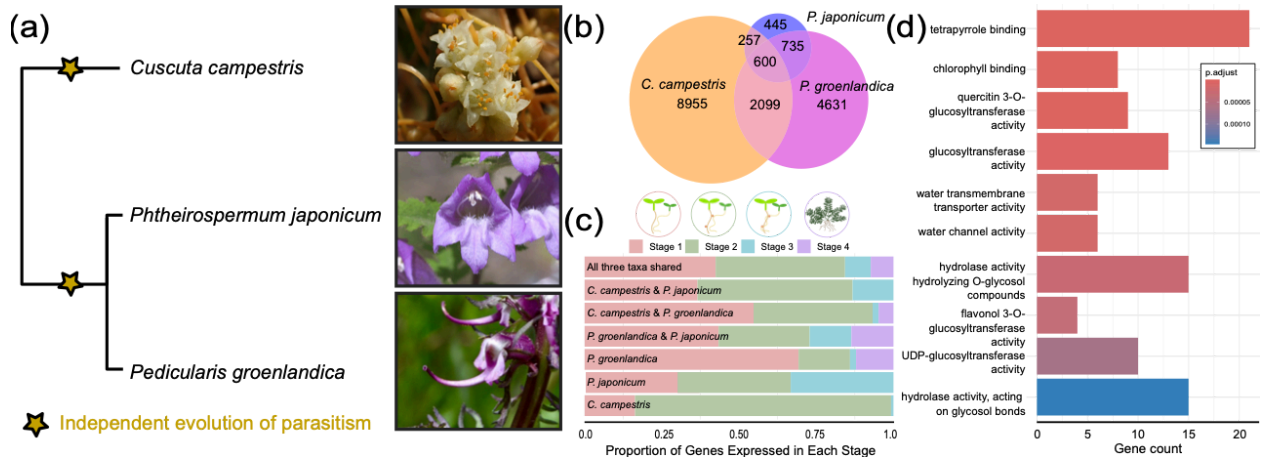

Fig. 6. Orthology of haustorial-associated genes in *Pedicularis groenlandica*, *Phtheirospermum japonicum*, and *Cuscuta campestris*. **a)** Cladogram showing the relationships between the three species, with two independent transitions to parasitism. Photographs of *C. campestris* and *P. japonicum* taken from iNaturalist with permission. (https://www.inaturalist.org/photos/62167474; https://www.inaturalist.org/observations/245056018) **b)** Venn diagram of the overlap in orthogroups among the three species. The number in each section is the sum of genes in all three species that make-up orthogroups in each category. **c)** Bar chart depicts the breakdown of genes in each of the Venn diagram categories by haustorial assay stage (1-4) in which they were differentially expressed in each species. *C. campestris* has a high amount of species-specific stage 2 genes. **d)** Molecular function GO enrichment analysis of the 600 genes in the orthogroups that overlap among all three species. Color of bars shows the adjusted p-value associated with enrichment, with red being more enriched and blue less enriched.

We evaluated the number of genes that made up the orthogroups in the three modern datasets. There were 600 haustoria-associated genes in the orthogroups that were shared by all three species: *P. groenlandica*, *P. japonicum*, and *C. campestris* (**Fig. 6b**). These genes included those involved in tetrapyrrole and chlorophyll binding, aquaporins, glucosyltransferases, hydrolases, and flavonoid-modifying enzymes (**Fig. 6d**). The lineage-specific orthogroups contained genes with distinct but complementary functions. In Orobanchaceae (overlap between *P. groenlandica* and *P. japonicum*), genes were enriched for functions related to cell wall modification, tropism, and photosynthesis/oxidative stress. In *C. campestris*, a holoparasite, genes were enriched for functions like external encapsulating structure organization, cell wall organization and modification, pectin catabolic process, and pattern specification.

Discussion

***Pedicularis groenlandica* genome –** Our *P. groenlandica* genome is a high-quality, chromosome-scale addition to the growing body of molecular data in the parasitic plant family Orobanchaceae. Including *P. groenlandica*, there are now eleven publicly-available chromosome-scale genomes in the family (Ma *et al.*, 2021; Xu *et al.*, 2022; Twyford *et al.*, 2024; Kim *et al.*, 2024; Chen *et al.*, 2024; Bürger *et al.*, 2025), and three in *Pedicularis* alone (Xu *et al.*, 2022; Fang *et al.* 2024). HiC data supported scaffolding the genome into eight chromosomes (**Fig. 2d**), which was consistent with our expectations based on available chromosome count data in *P. groenlandica* (Löve, 1982) and across *Pedicularis* (IPCN chromosome reports), including two chromosome-scale genomes (Xu et al., 2022; Fang et al., 2024). We report relatively constant gene density and GC content across the eight chromosomes and high transposable element (TE) density (**Fig. 2d**).

The *P. groenlandica* genome is highly repetitive (76.5% repeated), of which 44.5% were annotated as transposable elements (TE's). Differential accumulation of TE's drives changes in genome size in plants, and in parasitic plants in particular (Neumann *et al.*, 2021). Parasitic plants may disproportionately accumulate TE's relative to non-parasitic plants because genes "hitchhiking" on TE's can be horizontally transferred into parasitic plant genomes, driving genetic innovation, even in the face of increased rates of gene loss following the transition from autotrophy to heterotrophy (Cai, 2023). *P. groenlandica* has similarly high repeat content to other parasitic Orobanchaceae (*Phelipanche aegypitiaca*=84.4%, *Orobanche cumana*=79.8%, *Orobanche coreulescens*=86.3%), and higher repeat content than non-parasitic Orobanchaceae

638 (*Lindenbergia luchunensis*=30.7%, *Rehmannia glutinosa*=67%; Ma *et al.* 2021; Kim *et al.*,
639 2024). The relationship of genome repeat content to parasitism warrants further exploration,
640 particularly in a comparative context.
641 Xu et al. (2022) conducted a comparative genomic study of Orobanchaceae genomes,
642 which included the *P. cranolopha* genome in some analyses. They observed limited synteny
643 between *P. cranolopha* and two other Orobanchaceae genomes (*Lindenbergia luchunensis* and
644 *Orobanche cumana var. cumana*). Consistent with Xu et al.'s (2022) findings, *Pedicularis*
645 *groenlandica*'s eight chromosomes show clear synteny with *P. cranolopha*, with some small
646 inversions and translocations, but a high amount of rearrangement with respect to *O. cumana*
647 (**Fig. 2b**). From this, we conclude that *Pedicularis* genomes have undergone a major
648 re-organization since splitting from the common Orobanchaceae ancestor.
649
650 **Haustorial gene function and regulation in *P. groenlandica* –** Haustoria-associated genes
651 make-up 20.65% of all protein-coding genes in *P. groenlandica*, indicating haustorial
652 development and attachment leverages a wide range of molecular processes and elicits a
653 genome-wide response. Functions of genes across the haustorial developmental stages (**Fig.**
654 **4b**) were consistent with the functional categories we expected to be related to parasitism
655 based on previous haustorial RNAseq studies. For example, during Stage 1, we observed the
656 differential expression of genes involved in cell division and cell wall expansion, which likely is
657 related to the initiation of haustorial growth (Ishida *et al.*, 2016; Cui *et al.*, 2020). Stages 3 and 4
658 had similar expression patterns to each other, both showing enrichment for cellular tip
659 growth-related genes. Cui et al. (2016) found that cellular tip growth and cell elongation are
660 major mechanisms by which haustoria and functional haustorial hairs form in *Phtheirospermum*
661 *japonicum* (Orobanchaceae), a facultative hemi-parasite that is closely related to *Pedicularis*
662 within Orobanchaceae.
663 Similarly, the functional associations of haustoria-associated gene co-expression
664 networks included biological processes with known relevance to haustorial growth and invasion
665 (**Fig. 3c**). For example, flavonoid biosynthesis. Flavonoids are known to be related to haustoria
666 formation in *Triphysaria versicolor* (Albrecht *et al.*, 1999) and in the genus *Cuscuta* (Lozanova *et*
667 *al.*, 2025). We additionally identified a module of genes related to defense and immune
668 response (**Fig. 3c**), which we expect to include genes interacting with host defense pathways
669 during parasitic invasion. Hormone signaling and ion transport may also relate to host-parasite
670 cross-talk, and we saw enrichment of genes involved in auxin, ethylene, salicylic acid, and
671 phenylpropanoids, each of which have been linked to host-parasite signaling in other parasitic

plants (Ishida *et al.*, 2016; Cui *et al.*, 2020; Wakatake *et al.*, 2020; Mutuku *et al.*, 2021). Our results thus tell a consistent functional story about haustorial development compared to other parasitic lineages in which haustoria-associated genes have been identified, and we are confident that we have successfully captured the haustorial developmental process in *P. groenlandica*.

Pollen tubes and the evolution of haustoria-associated genes– Both Yang et al. (2015) and Yoshida et al. (2019) found that homologs of haustoria-associated genes in *Tryphisaria versicolor*, *Phelipanche aegypotiaca*, *Striga hermonthica*, and *S. asiatica* were enriched in pollen-related functions in model species like *Arabidopsis thaliana* and *Zea mays*. We hypothesized that this pattern results from the overlap in function of haustoria and the process of pollen tube growth which, like haustorial invasion, requires signal detection, growth through foreign tissue, and directed unidimensional cell growth. Sixty-one percent (3450/5635) of haustoria-associated genes were differentially expressed in both haustoria and pollen tubes, which represented a significant overlap (Fischer's Exact Test $P<10^{-70}$). This overlap was greater than any other non-parasitic tissue considered, including roots (**Fig. 4a**). The extent of the haustoria-pollen tube relationship was surprising, as haustoria-associated genes have been previously hypothesized to be co-opted from predominantly root-associated genetic pathways.

Pollen tube growth is known to require ethylene and auxin signaling (Guan *et al.*, 2013; Chen *et al.*, 2014; Weijers & Wagner, 2016; Cui *et al.*, 2020; Mou *et al.*, 2020) as well as genes in the expansin superfamily (Cosgrove, 1997; Sampedro & Cosgrove, 2005), all of which are also correlated with haustoria development (Yoshida *et al.*, 2016, 2019). In addition to high overlap in differential expressed genes among haustoria and pollen tubes, the two tissues shared the highest number of enriched regulatory motifs. The most common transcription factor family that shared enriched motifs interact with was ERF/DREB (**Fig. S4b**), which regulates ethylene signaling. Yoshida *et al.* (2016) argue that the co-option of the lateral root development program led to the evolution of haustoria across the twelve parasitic plant lineages, focusing in particular on pathways involved in auxin-biosynthesis and regulation. Across 5,635 haustoria-associated genes in *P. groenlandica*, 155 were involved in known auxin pathways, and of those, 62 auxin genes were additionally associated with pollen tubes, 18 were associated with roots, and 33 were associated with all three tissues. Despite known functioning of auxin pathways in roots, our results suggest that, in *P. groenlandica*, auxin functionality in haustoria has predominantly been co-opted from pollen tube-associated auxin pathways.

705 One explanation for the high proportion of haustoria-associated genes that were
706 differentially expressed in pollen tubes is that genes function pleiotropically in the two tissues.
707 We expect pleiotropy to give rise to divergence in *cis*-regulatory elements that mediate gene
708 expression, which is supported by our observation that a small proportion of enriched regulatory
709 motifs are shared between haustoria and non-parasitic tissues compared to protein-coding loci
710 (**Fig. 4b**). Further, genes being similarly grouped into coexpression modules (**Fig. 4c**) and
711 disparity in the direction of expression (**Fig. 4d**) among shared haustoria- and pollen-tube
712 associated genes is consistent with pleiotropy, and suggests that this pleiotropy may be
713 antagonistic in haustoria and pollen tubes (*i.e.* mutations in a pleiotropically functioning gene
714 may be beneficial in one tissue, but deleterious in another; Hoekstra & Coyne, 2007). Together,
715 these results suggest that divergence in regulation (*i.e.* gene expression) mediates the
716 variability in the functional processes of haustoria and pollen tubes.
717 A majority of the 5,635 haustoria-associated genes in *P. groenlandica* showed evidence
718 of association with pollen tubes, either because they were differentially expressed in pollen
719 tubes, nested within pollen tube-associated gene families, or both. Among haustoria-associated
720 genes that did not group into an orthogroup with a *P. groenlandica* paralog, 66% (1763/2664)
721 were themselves differentially expressed in pollen tubes; among those that did contain a paralog
722 in their orthogroup, 52% (1061/2054) were members of pollen tube-associated gene families
723 (*i.e.* at least one paralog was differentially expressed in pollen tubes). These patterns suggest
724 that haustoria have disproportionately co-opted functions from pollen tubes, and that pollen
725 tube-associated genes and gene families have been integral to the evolution of
726 haustoria-associated genes in *Pedicularis*. Although shared function cannot be inferred from
727 expression alone, our findings provide strong support for a close relationship between these two
728 tissue types that future studies can address experimentally to test pleiotropy more directly.
729
730 **Alternative explanations for the co-option of haustoria-associated genes–** Yang et al.
731 (2015) argue that haustoria-associated genes evolve through regulatory neofunctionalization
732 following ancient gene duplications, which they correlate with ancestral WGD's. If
733 haustoria-associated genes were derived from WGD's, we expected to identify an ancient
734 duplication in the evolutionary history of the majority of haustoria-associated genes in *P.*
735 *groenlandica* and likely haustoria-specific gene expression. In *P. groenlandica*, only 19.2% of
736 haustoria-associated genes showed evidence of diverging from non-haustoria-associated
737 paralogs following an ancient duplication. Furthermore, from examination of gene tree
738 topologies alone, the methodology employed by both Yang et al. (2015) and this study, whether

739 ancient duplications were derived from a WGD or another type of gene duplication (*i.e.* a
740 tandem duplication) that occurred in a shared common ancestor cannot be distinguished. We
741 show that the evolution of haustoria-specific expression is significantly more likely following a
742 recent duplication, and is not affected by the presence of ancient duplications. This is consistent
743 with the idea that recent, rather than ancient, duplications have facilitated neofunctionalization of
744 haustoria-specific genes. The predictive effect, however, is quite small, as the presence of a
745 recent paralog only makes it 7.6% more likely that a gene will exhibit haustoria-specific gene
746 expression.
747 Both regulatory neofunctionalization and pleiotropy are contexts in which new
748 phenotypes can evolve through variation in gene expression. Within our gene tree dataset, we
749 observed topologies and differential expression patterns in haustoria-associated and
750 non-haustoria-associated paralogs consistent with three, non-mutually exclusive, evolutionary
751 explanations for the advent of haustorial function: (1) pleiotropy (2) neofunctionalization
752 following a recent duplication, and (3) neofunctionalization following an ancient duplication. We
753 hypothesize that co-option of non-parasitic functions for haustorial development may initially
754 occur via pleiotropy, and subsequent recent (potentially lineage-specific) gene duplications have
755 given rise to paralogs primarily through neofunctionalization, perhaps to alleviate the burden of
756 pleiotropy. Fishman *et al.* (2025) provide evidence of neofunctionalization following a recent,
757 segmental tandem duplication in RGF orthologs in *Phtheirospermum japonicum*, consistent with
758 our hypothesis for haustoria-associated gene evolution. Further studies that validate
759 haustoria-associated gene functions in non-parasitic tissues and compare patterns of selection
760 acting on genes uniquely versus non-uniquely expressed in haustoria will be needed to
761 comprehensively investigate this hypothesis.
762
763 **Divergent pathways towards the evolution of haustoria—** We expected to identify a core set
764 of genes across Orobanchaceae that contribute to haustorial function in the family, derived in
765 Orobanchaceae's most recent common ancestor. Instead, although there is some overlap
766 among haustoria-associated genes across the parasitic plant lineages considered, a high
767 proportion of haustoria-associated genes are species-specific (**Fig. 6**). Yang et al. (2015)
768 similarly found that most haustoria-associated genes were lineage-specific when comparing
769 *Triphysaria versicolor, Striga hermonthica* and *Phelipanche aegyptiaca*. Unlike our analyses, the
770 species they examined span the full spectrum of parasitism, including a facultative
771 hemiparasite, obligate hemiparasite, and obligate holoparasite. Their results suggest that

772 hemiparasitic vs. holoparasitic haustorial function necessitates the recruitment of diverse sets of
773 genes, with relatively small overlap.
774 It was therefore surprising that even between the two closely-related facultative
775 hemiparasites *P. groenlandica* and *P. japonicum*, a high proportion of haustoria-associated
776 genes were species-specific. This result is particularly interesting in light of our findings that 1)
777 *Pedicularis* have highly rearranged genomes with respect to other Orobanchaceae and 2)
778 recent duplications predict whether a haustoria-associated paralog is differentially expressed
779 only in haustoria. Together, these results suggest that since the evolution of haustoria in the
780 common ancestor of Orobanchaceae, a substantial amount of variation has evolved among
781 descendant lineages in the recruitment of genes into haustoria-associated functions. Many
782 aspects of the biology of these organisms have likely impacted this process. For example,
783 *Pedicularis* has experienced an adaptive radiation since the Miocene, where it now comprises
784 >600 species distributed mostly throughout montane and arctic ecosystems (Eaton & Ree,
785 2013). Whether *Pedicularis* has evolved variation in haustoria-associated regulatory
786 neofunctionalization faster than other parasitic lineages will require further comparative
787 analyses, examining the distribution of haustoria-associated genes with respect to synteny. The
788 closely related genus *Castilleja* offers an opportunity for comparison with a similarly large and
789 diverse clade (Li *et al.*, 2019).
790 Because transcriptomes of *Cuscuta campestris* haustoria were sequenced more recently
791 (Bawin *et al.*, 2022, 2024), neither Westwood et al. (2012) nor Yang et al. (2015) included a
792 convergently evolved haustoria from outside Orobanchaceae in their comparative transcriptomic
793 analyses. Using Bawin et al.'s (2024) haustoria RNAseq data, we were able to compare
794 haustoria-associated genes in Orobanchaceae and *Cuscuta*. There were a number of haustorial
795 genes that occurred in common orthogroups among *P. groenlandica*, *P. japonicum*, and *C.*
796 *campestris*. The shared orthogroups among all three lineages included genes with functions
797 related largely to water transfer. Both *P. groenlandica* and *P. japonicum* are hemiparasitic,
798 meaning their haustoria invade only the xylem of a host plant in order to siphon water (Yoshida
799 *et al.*, 2016). In contrast, *C. campestris*, as a holoparasite, has haustoria that penetrate both the
800 xylem and phloem of a host (Yoshida *et al.*, 2016). The overlap in genes that function in
801 tetrapyrrole binding, glucosyltransferase, and water transmembrane/channel molecular
802 pathways (**Fig. 6D**), indicates potential commonality in the way that hemi- and holoparasites
803 invade xylem and transfer water from their hosts. This is consistent with the hypothesis that
804 holoparasitism evolves subsequent to the evolution of hemiparasitism, and that the first

haustoria in parasitic lineages likely resembled the lateral haustoria of hemiparasites (Westwood et al. 2010).

Conclusions

This study presents strong evidence for the importance of pollen tube-associated genetic pathways in the evolution of haustoria in *P. groenlandica*. We additionally highlight the need to evaluate diverse mechanistic explanations for the co-option of genes for haustorial function in parasitic plants, and, more broadly, the ways in which changes in gene expression can contribute to the evolution of novel phenotypes. Finally, although the data available from the Parasitic Plant Genome Project represented a huge advance in parasitic plant genetic research, these data no longer meet the expectations for modern RNA sequencing experiments, including the expected level of replication (three biological replicates per stage), that is available in the *P. groenlandica*, *P. japonicum*, and *C. campestris* datasets. We underscore the need for additional high-quality genome and haustorial RNA datasets in order to conduct more comprehensive comparative studies of haustorial gene evolution within Orobanchaceae and across parasitic plant lineages.

Acknowledgements

We thank B. Stokes for her help with tissue collection at RMBL, and A. Cisse for assistance with both fieldwork and seed germination for haustorial assays. We additionally thank N. Gershberg for his assistance and advice related to plant care, and J. Reithel and R. Williams for their assistance in fieldwork at RMBL. We thank I. Overcast, J. Leung, Y. Yang, and R. Rampalli, and D. Timerman for their feedback on the manuscript.

This work was supported by the National Science Foundation (NSF DEB-2046813) awarded to D.E and, the RMBL Graduate Student Grant awarded to R.O.C., and the Botanical Society of America Graduate Student Research Award awarded to R.O.C.

Competing interests

We declare no competing interests.

Author contributions

R.O.C and D.E. contributed equally to study design. R.O.C. collected all data and conducted all differential expression analyses. R.O.C. and A.C. did gene co-expression network and motif enrichment analyses. R.O.C. and D.E. conducted the gene duplication-related analyses. R.O.C., D.E., A.C., and L.C. contributed to the writing of the manuscript.

Data availability

Herbarium vouchers for *P. groenlandica* were deposited at Rocky Mountain Biological Laboratory (RMBL) herbarium (voucher RMBL0007650) and New York Botanical Garden William and Lynda Steere Herbarium. Due to a backlog of vouchers, our specimens had not yet been processed at the time of publication. They will be able to be found using the collector's and species' names (R. Cohen) after they have been fully processed by NYBG.

All genomic and transcriptomic data will be available on NCBI, and we will provide the SRAs. Dataframes containing haustorial gene expression and haustoria-associated gene orthology data and the jupyter notebook containing code for gene tree analyses will be available on Dryad.

References

Abbas F, Ke Y, Yu R, Yue Y, Amanullah S, Jahangir MM, Fan Y. **2017**. Volatile terpenoids: multiple functions, biosynthesis, modulation and manipulation by genetic engineering. *Planta* **246**: 803–816.

Albrecht H, Yoder JI, Phillips DA. **1999**. Flavonoids Promote Haustoria Formation in the Root Parasite *Triphysaria versicolor*. *Plant Physiology* **119**: 585–592.

Andrews, S. 2010. FastQC: A Quality Control Tool for High Throughput Sequence Data [Online]. Available online at: http://www.bioinformatics.babraham.ac.uk/projects/fastqc/

Bailey TL, Boden M, Buske FA, Frith M, Grant CE, Clementi L, Ren J, Li WW, Noble WS. **2009**. MEME Suite: tools for motif discovery and searching. *Nucleic Acids Research* **37**: W202–W208.

Bawin T, Bruckmüller J, Olsen S, Krause K. **2022**. A host-free transcriptome for haustoriogenesis in Cuscuta campestris: Signature gene expression identifies markers of successive development stages. *Physiologia Plantarum* **174**: e13628.

Bawin T, Didriksen A, Faehn C, Olsen S, Sørensen I, Rose JKC, Krause K. **2024**. Cuscuta campestris fine-tunes gene expression during haustoriogenesis as an adaptation to different hosts. *Plant Physiology* **194**: 258–273.

von Besser K, Frank AC, Johnson MA, Preuss D. **2006**. Arabidopsis HAP2 (GCS1) is a sperm-specific gene required for pollen tube guidance and fertilization. *Development (Cambridge, England)* **133**: 4761–4769.

Brůna T, Lomsadze A, Borodovsky M. **2024**. GeneMark-ETP significantly improves the accuracy of automatic annotation of large eukaryotic genomes. *Genome Research* **34**: 757–768.

Bürger M, Soco CF, García MA, Seto Y, Leyva A. **2025**. Three Orobanche genomes reveal distinct molecular repertoires in species with different host ranges. *Plant and Cell Physiology*: pcaf047.

Cai L. **2023**. Rethinking convergence in plant parasitism through the lens of molecular and population genetic processes. *American Journal of Botany* **110**: e16174.

Chen B-Z, Li D-W, Luo K-Y, Jiu S-T, Dong X, Wang W-B, Li X-Z, Hao T-T, Lei Y-H, Guo D-Z, *et al.* 2024. Chromosome-level assembly of Lindenbergia philippensis and comparative genomic analyses shed light on genome evolution in Lamiales. *Frontiers in Plant Science* **15**.

Chen Y, Zou M, Cao Y. **2014**. Transcriptome analysis of the Arabidopsis semi-in vivo pollen tube guidance system uncovers a distinct gene expression profile. *Journal of Plant Biology* **57**: 93–105.

Cheng H, Concepcion GT, Feng X, Zhang H, Li H. **2021**. Haplotype-resolved de novo assembly using phased assembly graphs with hifiasm. *Nature Methods* **18**: 170–175.

Chomentowska A, Raimondeau P, Wei L, Jose EGD, Dauerman SG, Davis VZ, Moreira-Muñoz A, Peralta IE, Edwards EJ. **2025**. A high-quality genome of the Atacama Desert plant Cistanthe cachinalensis and its photosynthetic behavior related to drought and life history. *New Phytologist* **247**: 388–407.

Cohen RO, Cisse A, Jones JU, Williams JH, Eaton DAR. **2025**. Phylogeny does not predict the outcome of heterospecific pollen–pistil interactions in a species-rich alpine plant community. *American Journal of Botany* **n/a**: e70004.

Cosgrove DJ. **1997**. Creeping walls, softening fruit, and penetrating pollen tubes: The growing roles of expansins | PNAS.

Cui S, Kubota T, Nishiyama T, Ishida JK, Shigenobu S, Shibata TF, Toyoda A, Hasebe M, Shirasu K, Yoshida S. **2020**. Ethylene signaling mediates host invasion by parasitic plants. *Science Advances* **6**: eabc2385.

Cui S, Wakatake T, Hashimoto K, Saucet SB, Toyooka K, Yoshida S, Shirasu K. **2016**. Haustorial Hairs Are Specialized Root Hairs That Support Parasitism in the Facultative Parasitic Plant Phtheirospermum japonicum. *Plant Physiology* **170**: 1492–1503.

Daher FB, Geitmann A. **2012**. Actin depolymerizing factors ADF7 and ADF10 play distinct roles during pollen development and pollen tube growth. *Plant Signaling & Behavior* **7**: 879–881.

DiGiovanni JP, Wysocki WP, Burke SV, Duvall MR, Barber NA. **2017**. The role of hemiparasitic plants: influencing tallgrass prairie quality, diversity, and structure. *Restoration Ecology* **25**: 405–413.

Dobin A, Davis CA, Schlesinger F, Drenkow J, Zaleski C, Jha S, Batut P, Chaisson M, Gingeras TR. **2013**. STAR: ultrafast universal RNA-seq aligner. *Bioinformatics (Oxford, England)* **29**: 15–21.

Durand NC, Shamim MS, Machol I, Rao SSP, Huntley MH, Lander ES, Aiden EL. **2016**. Juicer Provides a One-Click System for Analyzing Loop-Resolution Hi-C Experiments. *Cell Systems* **3**: 95–98.

Eaton DAR. **2020**. Toytree: A minimalist tree visualization and manipulation library for Python. *Methods in Ecology and Evolution* **11**: 187–191.

Eaton DAR, Fenster CB, Hereford J, Huang S-Q, Ree RH. **2012**. Floral diversity and community structure in Pedicularis (Orobanchaceae). *Ecology* **93**: S182–S194.

Eaton DAR, Ree RH. **2013**. Inferring Phylogeny and Introgression using RADseq Data: An Example from Flowering Plants (Pedicularis: Orobanchaceae). *Systematic Biology* **62**: 689–706.

Emms DM, Kelly S. **2019**. OrthoFinder: phylogenetic orthology inference for comparative genomics. *Genome Biology* **20**: 238.

Fang L, Li M, Zhang J, Jia C, Qiang Y, He X, Liu T, Zhou Q, Luo D, Han Y, *et al.* 2024. Chromosome-level genome assembly of Pedicularis kansuensis illuminates genome evolution of facultative parasitic plant. *Molecular Ecology Resources* **24**: e13966.

Fernández-Aparicio M, Reboud X, Gibot-Leclerc S. **2016**. Broomrape Weeds. Underground Mechanisms of Parasitism and Associated Strategies for their Control: A Review. *Frontiers in Plant Science* **7**.

Fishman MR, Greifenhagen A, Wakatake T, Laohavisit A, Hiroyama R, Masuda S, Shibata A, Yoshida S, Shirasu K. **2025**. Neofunctionalized RGF pathways drive haustorial organogenesis in parasitic plants. *Science Advances* **11**: eadw3965.

Flynn JM, Hubley R, Goubert C, Rosen J, Clark AG, Feschotte C, Smit AF. **2020**. RepeatModeler2 for automated genomic discovery of transposable element families. *Proceedings of the National Academy of Sciences* **117**: 9451–9457.

Furuta KM, Xiang L, Cui S, Yoshida S. **2021**. Molecular dissection of haustorium development in Orobanchaceae parasitic plants. *Plant Physiology* **186**: 1424–1434.

Gabriel L, Brůna T, Hoff KJ, Ebel M, Lomsadze A, Borodovsky M, Stanke M. **2024**. BRAKER3: Fully automated genome annotation using RNA-seq and protein evidence with GeneMark-ETP, AUGUSTUS, and TSEBRA. *Genome Research* **34**: 769–777.

Gao Q-F, Gu L-L, Wang H-Q, Fei C-F, Fang X, Hussain J, Sun S-J, Dong J-Y, Liu H, Wang Y-F. **2016**. Cyclic nucleotide-gated channel 18 is an essential Ca2+ channel in pollen tube tips for pollen tube guidance to ovules in Arabidopsis. *Proceedings of the National Academy of Sciences of the United States of America* **113**: 3096–3101.

Gilman IS, Moreno-Villena JJ, Lewis ZR, Goolsby EW, Edwards EJ. **2022**. Gene co-expression reveals the modularity and integration of C4 and CAM in Portulaca. *Plant Physiology* **189**: 735–753.

Grant V. **1994**. Modes and Origins of Mechanical and Ethological Isolation in Angiosperms. *Proceedings of the National Academy of Sciences of the United States of America* **91**: 3–10.

Guan Y, Guo J, Li H, Yang Z. **2013**. Signaling in Pollen Tube Growth: Crosstalk, Feedback, and Missing Links. *Molecular Plant* **6**: 1053–1064.

Hoekstra HE, Coyne JA. **2007**. THE LOCUS OF EVOLUTION: EVO DEVO AND THE GENETICS OF ADAPTATION. *Evolution* **61**: 995–1016.

Ishida JK, Wakatake T, Yoshida S, Takebayashi Y, Kasahara H, Wafula E, dePamphilis CW, Namba S, Shirasu K. **2016**. Local Auxin Biosynthesis Mediated by a YUCCA Flavin Monooxygenase Regulates Haustorium Development in the Parasitic Plant Phtheirospermum japonicum. *The Plant Cell* **28**: 1795–1814.

Jhu M-Y, Farhi M, Wang L, Zumstein K, Sinha NR. **2021**. Investigating Host and Parasitic Plant Interaction by Tissue-Specific Gene Analyses on Tomato and Cuscuta campestris Interface at Three Haustorial Developmental Stages.

Joel DM, Gressel J, Musselman LJ (Eds.). **2013**. *Parasitic Orobanchaceae*. Berlin, Heidelberg: Springer Berlin Heidelberg.

Kim B, Jhang SY, Koh B, Kim S, Chi W-J, Park J-M, Lim CE, Hong Y, Kim H, Yu J, *et al.* **2024**. Chromosome-level genome assembly of Korean holoparasitic plants, Orobanche coerulescens. *Scientific Data* **11**: 714.

Kirschner GK, Xiao TT, Jamil M, Al-Babili S, Lube V, Blilou I. **2023**. A roadmap of haustorium morphogenesis in parasitic plants. *Journal of Experimental Botany* **74**: 7034–7044.

Kokla A, Leso M, Zhang X, Simura J, Cui S, Ljung K, Yoshida S, Melnyk CW. **2021**. Nitrates increase abscisic acid levels to regulate haustoria formation in the parasitic plant Phtheirospermum japonicum. : 2021.06.15.448499.

Kovaka S, Zimin AV, Pertea GM, Razaghi R, Salzberg SL, Pertea M. **2019**. Transcriptome assembly from long-read RNA-seq alignments with StringTie2. *Genome Biology* **20**: 278.

Kozlov AM, Darriba D, Flouri T, Morel B, Stamatakis A. **2019**. RAxML-NG: a fast, scalable and user-friendly tool for maximum likelihood phylogenetic inference. *Bioinformatics* **35**: 4453–4455.

Krueger F. **2015**. Trim Galore!: A wrapper around Cutadapt and FastQC to consistently apply adapter and quality trimming to FastQ files, with extra functionality for RRBS data. *Babraham Institute*.

Lamesch P, Berardini TZ, Li D, Swarbreck D, Wilks C, Sasidharan R, Muller R, Dreher K, Alexander DL, Garcia-Hernandez M, *et al.* **2012**. The Arabidopsis Information Resource (TAIR): improved gene annotation and new tools. *Nucleic Acids Research* **40**: D1202–D1210.

Langfelder P, Horvath S. **2008**. WGCNA: an R package for weighted correlation network analysis. *BMC Bioinformatics* **9**: 559.

Li X, Feng T, Randle C, Schneeweiss GM. **2019**. Phylogenetic Relationships in Orobanchaceae Inferred From Low-Copy Nuclear Genes: Consolidation of Major Clades and Identification of a Novel Position of the Non-photosynthetic Orobanche Clade Sister to All Other Parasitic Orobanchaceae. *Frontiers in Plant Science* **10**: 902.

Liao Y, Smyth GK, Shi W. **2014**. featureCounts: an efficient general purpose program for assigning sequence reads to genomic features. *Bioinformatics (Oxford, England)* **30**: 923–930.

Löve Á. **1982**. IOPB Chromosome Number Reports LXXIV. *Taxon* **31**: 119–128.

Love MI, Huber W, Anders S. **2014**. Moderated estimation of fold change and dispersion for RNA-seq data with DESeq2. *Genome Biology* **15**: 550.

Lozanova V, Teofanova D, Chakarova B, Rusanov K, Pachedjieva K, Tosheva A, Zagorcheva T, Zagorchev L. **2025**. The Antioxidant Properties of Extracts of Cuscuta spp. Depend on the Parasite and the Host Species. *Antioxidants* **14**: 761.

Lyko P, Wicke S. **2021**. Genomic reconfiguration in parasitic plants involves considerable gene losses alongside global genome size inflation and gene births. *Plant Physiology* **186**: 1412–1423.

Ma L, Dong C, Song C, Wang X, Zheng X, Niu Y, Chen S, Feng W. **2021**. De novo genome assembly of the potent medicinal plant Rehmannia glutinosa using nanopore technology. *Computational and Structural Biotechnology Journal* **19**: 3954–3963.

Macior LW. **1968**. Pollination Adaptation in Pedicularis Groenlandica. *American Journal of Botany* **55**: 927–932.

Masumoto N, Suzuki Y, Cui S, Wakazaki M, Sato M, Kumaishi K, Shibata A, Furuta KM, Ichihashi Y, Shirasu K, *et al.* 2021. Three-dimensional reconstructions of haustoria in two parasitic plant species in the Orobanchaceae. *Plant Physiology* **185**: 1429–1442.

Moore RC, Purugganan MD. **2005**. The evolutionary dynamics of plant duplicate genes. *Current Opinion in Plant Biology* **8**: 122–128.

Morel B, Kozlov AM, Stamatakis A, Szöllősi GJ. **2020**. GeneRax: A Tool for Species-Tree-Aware Maximum Likelihood-Based Gene Family Tree Inference under Gene Duplication, Transfer, and Loss. *Molecular Biology and Evolution* **37**: 2763–2774.

Mou W, Kao Y-T, Michard E, Simon AA, Li D, Wudick MM, Lizzio MA, Feijó JA, Chang C. **2020**. Ethylene-independent signaling by the ethylene precursor ACC in Arabidopsis ovular pollen tube attraction. *Nature Communications* **11**: 4082.

Mutuku JM, Cui S, Yoshida S, Shirasu K. **2021**. Orobanchaceae parasite–host interactions. *New Phytologist* **230**: 46–59.

Neumann P, Oliveira L, Čížková J, Jang T-S, Klemme S, Novák P, Stelmach K, Koblížková A, Doležel J, Macas J. **2021**. Impact of parasitic lifestyle and different types of centromere organization on chromosome and genome evolution in the plant genus Cuscuta. *New Phytologist* **229**: 2365–2377.

Niklas KJ, Kutschera U. **2009**. The evolutionary development of plant body plans. *Functional Plant Biology* **36**: 682–695.

Ohno S. **1970**. *Evolution by Gene Duplication*. Springer Science & Business Media.

Pan X, Chang Y, Li C, Qiu X, Cui X, Meng F, Zhang S, Li X, Lu S. **2023**. Chromosome-level genome assembly of Salvia miltiorrhiza with orange roots uncovers the role of Sm2OGD3 in catalyzing 15,16-dehydrogenation of tanshinones. *Horticulture Research* **10**: uhad069.

Pertea G, Pertea M. **2020**. GFF Utilities: GffRead and GffCompare. *F1000Research* **9**: ISCB Comm J-304.

Piehl MA. **1963**. Mode of Attachment, Haustorium Structure, and Hosts of Pedicularis Canadensis. *American Journal of Botany* **50**: 978–985.

Press M, Graves J. **1995**. *Parasitic Plants*. Springer Science & Business Media.

Quinlan AR. **2014**. BEDTools: The Swiss-Army Tool for Genome Feature Analysis. *Current Protocols in Bioinformatics* **47**: 11.12.1-11.12.34.

Rauluseviciute I, Riudavets-Puig R, Blanc-Mathieu R, Castro-Mondragon JA, Ferenc K, Kumar V, Lemma RB, Lucas J, Chèneby J, Baranasic D, *et al.* 2024. JASPAR 2024: 20th anniversary of the open-access database of transcription factor binding profiles. *Nucleic Acids Research* **52**: D174–D182.

Ren Y-Q, Guan K-Y, Li A-R, Hu X-J, Zhang L. **2010**. Host Dependence and Preference of the Root Hemiparasite, Pedicularis cephalantha Franch. (Orobanchaceae). *Folia Geobotanica* **45**: 443–455.

Sampedro J, Cosgrove DJ. **2005**. The expansin superfamily. *Genome Biology* **6**: 242.

Seabold, S. and Perktold, J. 2010. Statsmodels: Econometric and Modeling with Python. 9th Python in Science Conference, Austin, 28 June-3 July, 2010, 57-61. https://doi.org/10.25080/Majora-92bf1922-011

Seppey M, Manni M, Zdobnov EM. **2019**. BUSCO: Assessing Genome Assembly and Annotation Completeness. In: Kollmar M, ed. Methods in Molecular Biology. Gene Prediction: Methods and Protocols. New York, NY: Springer, 227–245.

Smit, AFA, Hubley, R & Green, P. 2013-2015. RepeatMasker Open-4.0. <http://www.repeatmasker.org>.

Stanke M, Diekhans M, Baertsch R, Haussler D. **2008**. Using native and syntenically mapped cDNA alignments to improve de novo gene finding. *Bioinformatics* **24**: 637–644.

Stanke M, Schöffmann O, Morgenstern B, Waack S. **2006**. Gene prediction in eukaryotes with a generalized hidden Markov model that uses hints from external sources. *BMC Bioinformatics* **7**: 62.

Sun G, Xu Y, Liu H, Sun T, Zhang J, Hettenhausen C, Shen G, Qi J, Qin Y, Li J, *et al.* 2018. Large-scale gene losses underlie the genome evolution of parasitic plant Cuscuta australis. *Nature Communications* **9**: 2683.

Takei S, Otani M, Ishikawa T, Suzuki T, Okabe S, Nishiyama K, Kawakami N, Seto Y. **2024**. Highly Sensitive Strigolactone Perception by a Divergent Clade KAI2 Receptor in a Facultative Root Parasitic Plant, Phtheirospermum japonicum. *Plant & Cell Physiology* **65**: 1958–1968.

Tang H, Krishnakumar V, Zeng X, Xu Z, Taranto A, Lomas JS, Zhang Y, Huang Y, Wang Y, Yim WC, *et al.* 2024. JCVI: A versatile toolkit for comparative genomics analysis. *iMeta* **3**: e211.

Tong Z-Y, Huang S-Q. **2016**. Pre- and post-pollination interaction between six co-flowering Pedicularis species via heterospecific pollen transfer. *New Phytologist* **211**: 1452–1461.

Twyford AD, Royal Botanic Garden Edinburgh Genome Acquisition Lab, Darwin Tree of Life Barcoding collective, Wellcome Sanger Institute Tree of Life Management, Samples and Laboratory team, Wellcome Sanger Institute Scientific Operations: Sequencing Operations, Wellcome Sanger Institute Tree of Life Core Informatics team, Tree of Life Core Informatics collective, Darwin Tree of Life Consortium. **2024**. The genome sequence of the confused eyebright, Euphrasia confusa Pugsley. *Wellcome Open Research* **9**: 662.

Vogel A, Schwacke R, Denton AK, Usadel B, Hollmann J, Fischer K, Bolger A, Schmidt MH-W, Bolger ME, Gundlach H, *et al.* 2018. Footprints of parasitism in the genome of the parasitic flowering plant Cuscuta campestris. *Nature Communications* **9**: 2515.

Wakatake T, Ogawa S, Yoshida S, Shirasu K. **2020**. An auxin transport network underlies xylem bridge formation between the hemi-parasitic plant Phtheirospermum japonicum and host Arabidopsis. *Development* **147**: dev187781.

Wang Y, Yao R, Du X, Guo L, Chen L, Xie D, Smith SM. **2021**. Molecular basis for high ligand sensitivity and selectivity of strigolactone receptors in Striga. *Plant Physiology* **185**: 1411–1428.

Weijers D, Wagner D. **2016**. Transcriptional Responses to the Auxin Hormone. *Annual Review of Plant Biology* **67**: 539–574.

Westwood JH, dePamphilis CW, Das M, Fernández-Aparicio M, Honaas LA, Timko MP, Wafula EK, Wickett NJ, Yoder JI. **2012**. The Parasitic Plant Genome Project: New Tools for Understanding the Biology of Orobanche and Striga. *Weed Science* **60**: 295–306.

Westwood JH, Yoder JI, Timko MP, dePamphilis CW. **2010**. The evolution of parasitism in plants. *Trends in Plant Science* **15**: 227–235.

Wu T, Hu E, Xu S, Chen M, Guo P, Dai Z, Feng T, Zhou L, Tang W, Zhan L, *et al.* 2021. clusterProfiler 4.0: A universal enrichment tool for interpreting omics data. *The Innovation* **2**.

Xu Y, Zhang J, Ma C, Lei Y, Shen G, Jin J, Eaton DAR, Wu J. **2022**. Comparative genomics of orobanchaceous species with different parasitic lifestyles reveals the origin and stepwise evolution of plant parasitism. *Molecular Plant* **15**: 1384–1399.

Yang Z, Wafula EK, Honaas LA, Zhang H, Das M, Fernandez-Aparicio M, Huang K, Bandaranayake PCG, Wu B, Der JP, *et al.* 2015. Comparative Transcriptome Analyses Reveal Core Parasitism Genes and Suggest Gene Duplication and Repurposing as Sources of Structural Novelty. *Molecular Biology and Evolution* **32**: 767–790.

Ye J, McGinnis S, Madden TL. **2006**. BLAST: improvements for better sequence analysis. *Nucleic Acids Research* **34**: W6–W9.

Yoshida S, Cui S, Ichihashi Y, Shirasu K. **2016**. The Haustorium, a Specialized Invasive Organ in Parasitic Plants. *Annual Review of Plant Biology* **67**: 643–667.

Yoshida S, Kim S, Wafula EK, Tanskanen J, Kim Y-M, Honaas L, Yang Z, Spallek T, Conn CE, Ichihashi Y, *et al.* 2019. Genome Sequence of Striga asiatica Provides Insight into the Evolution of Plant Parasitism. *Current Biology* **29**: 3041-3052.e4.

Zdobnov EM, Kuznetsov D, Tegenfeldt F, Manni M, Berkeley M, Kriventseva EV. **2021**. OrthoDB in 2020: evolutionary and functional annotations of orthologs. *Nucleic Acids Research* **49**: D389–D393.

Zhang X, Berkowitz O, Teixeira da Silva J, Zhang M, Ma G, Whelan J, Duan J. **2015**. RNA-Seq analysis identifies key genes associated with haustorial development in the root hemiparasite Santalum album. *Frontiers in Plant Science* **6**.

Zhou C, McCarthy SA, Durbin R. **2023**. YaHS: yet another Hi-C scaffolding tool. *Bioinformatics* **39**: btac808.

Zhou Y, Zhang Z, Bao Z, Li H, Lyu Y, Zan Y, Wu Y, Cheng L, Fang Y, Wu K, *et al.* 2022. Graph pangenome captures missing heritability and empowers tomato breeding. *Nature* **606**: 527–534. formation

Stage 1

P. groenlandica roots 24 hours post exposure to host

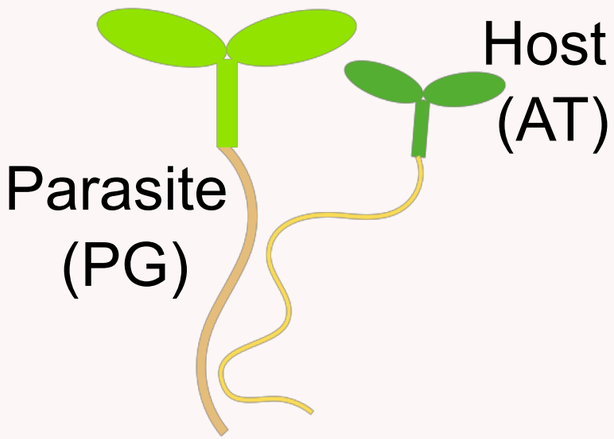

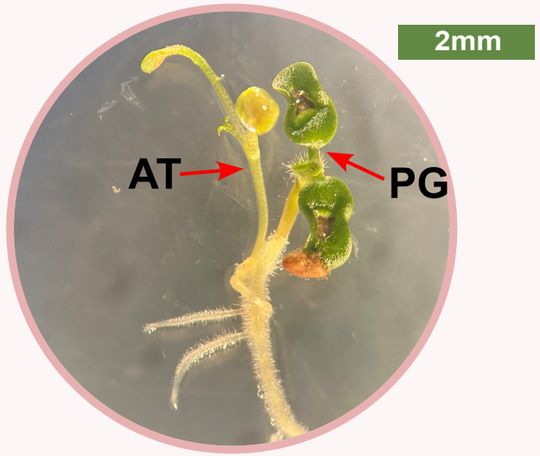

Stage 2

Haustoria swelling

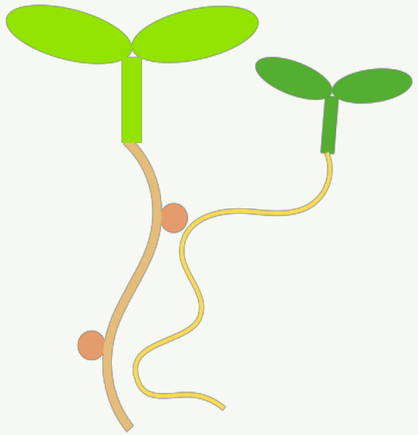

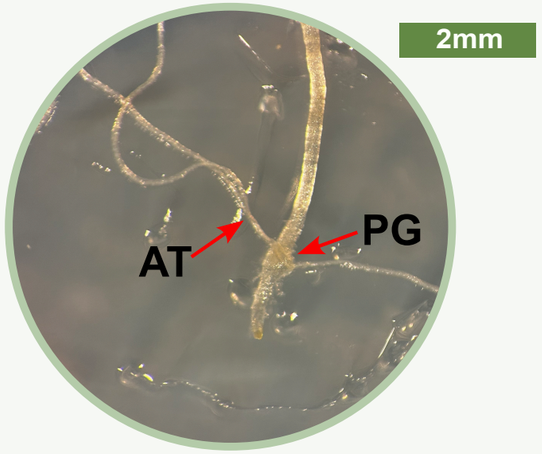

Stage 3

Haustoria attached and penetrating host

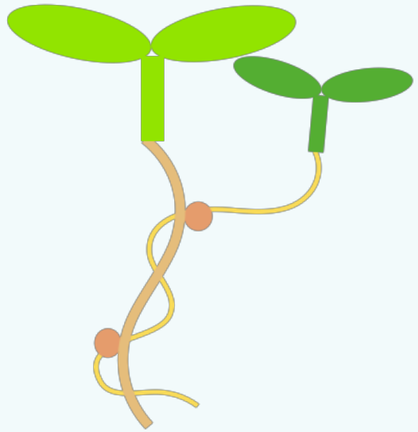

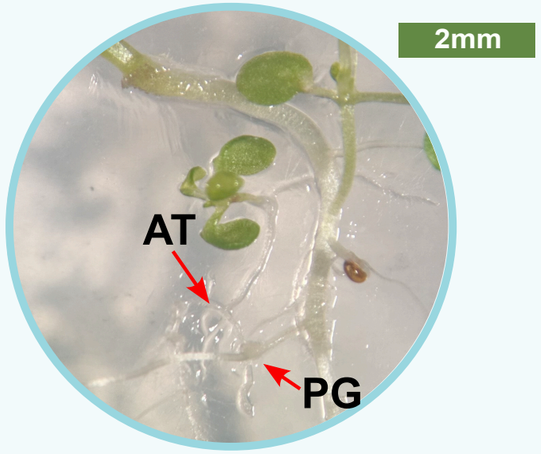

Stage 4

Mature, field-collected haustoria

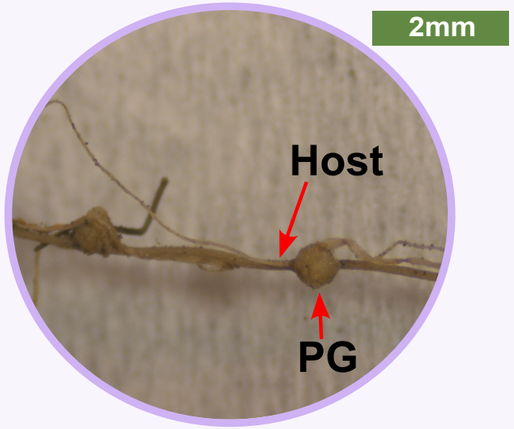

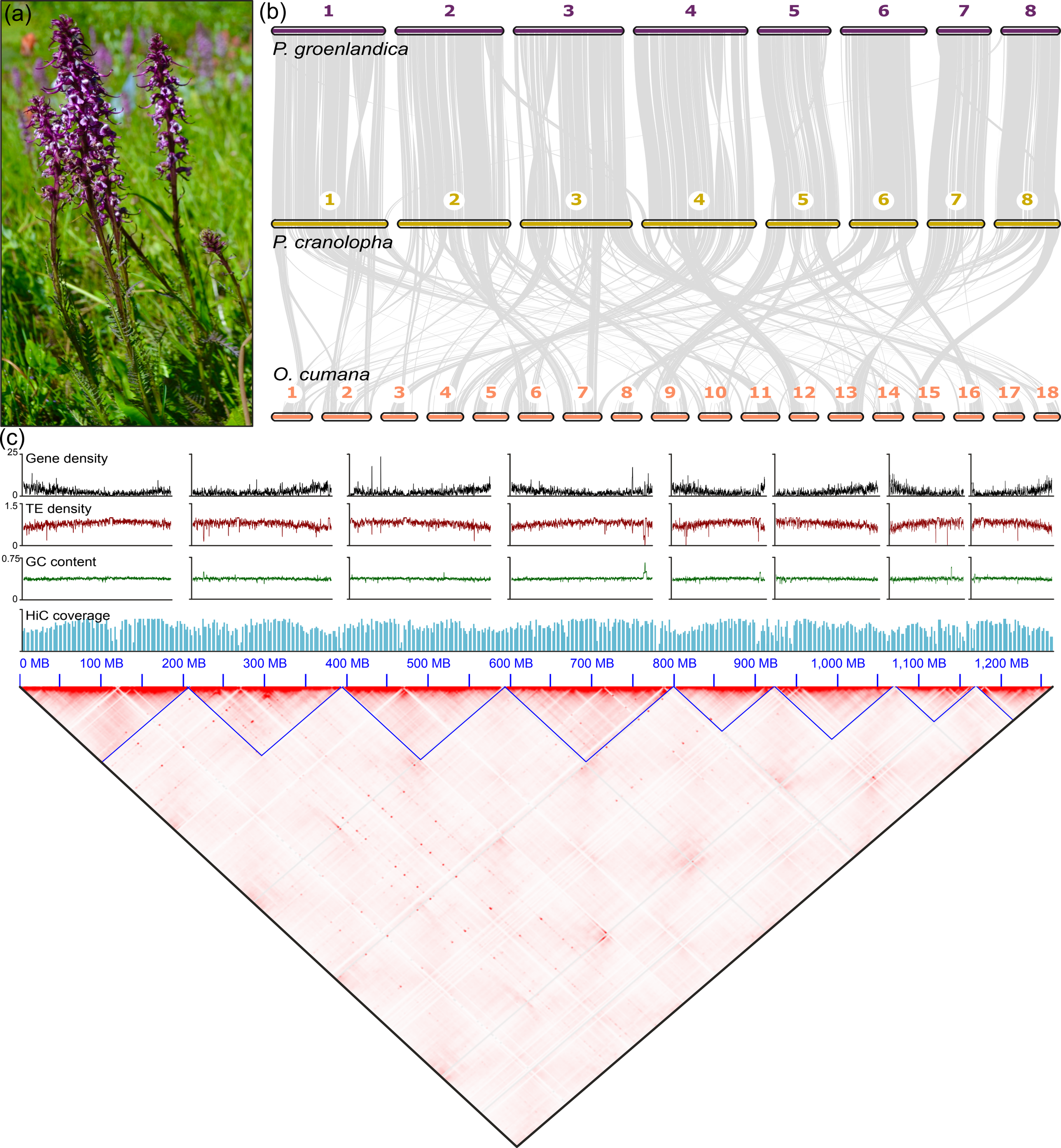
(a)
(b)
1
2
3
4
5
6
7
8
P. groenlandica
P. cranolopha
O. cumana
1 2 3 4 5 6 7 8 9 10 11 12 13 14 15 16 17 18
(c)
Gene density
25
0
TE density
1.5
0
GC content
0.75
0
HiC coverage
0 MB
100 MB
200 MB
300 MB
400 MB
500 MB
600 MB
700 MB
800 MB
900 MB
1,000 MB
1,100 MB
1,200 MB

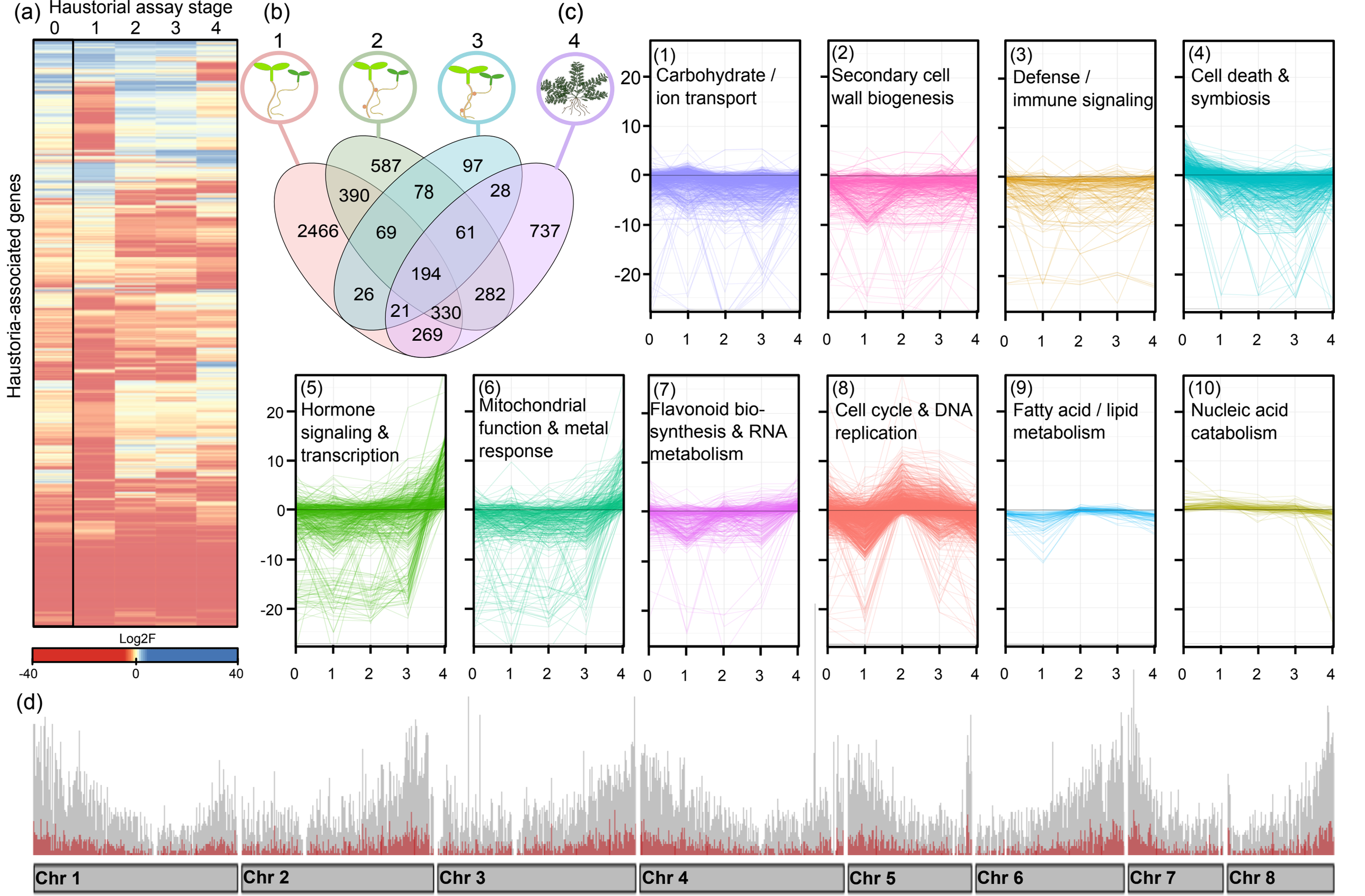
(a)
Haustorial assay stage
0 1 2 3 4
Haustoria-associated genes
Log2F
-40 0 40
(b)
1 2 3 4
587
97
390
78
28
2466
69
61
737
194
26
282
21
330
269
(c)
(1) Carbohydrate / ion transport
(2) Secondary cell wall biogenesis
(3) Defense / immune signaling
(4) Cell death & symbiosis
(5) Hormone signaling & transcription
(6) Mitochondrial function & metal response
(7) Flavonoid bio-synthesis & RNA metabolism
(8) Cell cycle & DNA replication
(9) Fatty acid / lipid metabolism
(10) Nucleic acid catabolism
20 10 0 -10 -20
0 1 2 3 4
(d)
Chr 1
Chr 2
Chr 3
Chr 4
Chr 5
Chr 6
Chr 7
Chr 8

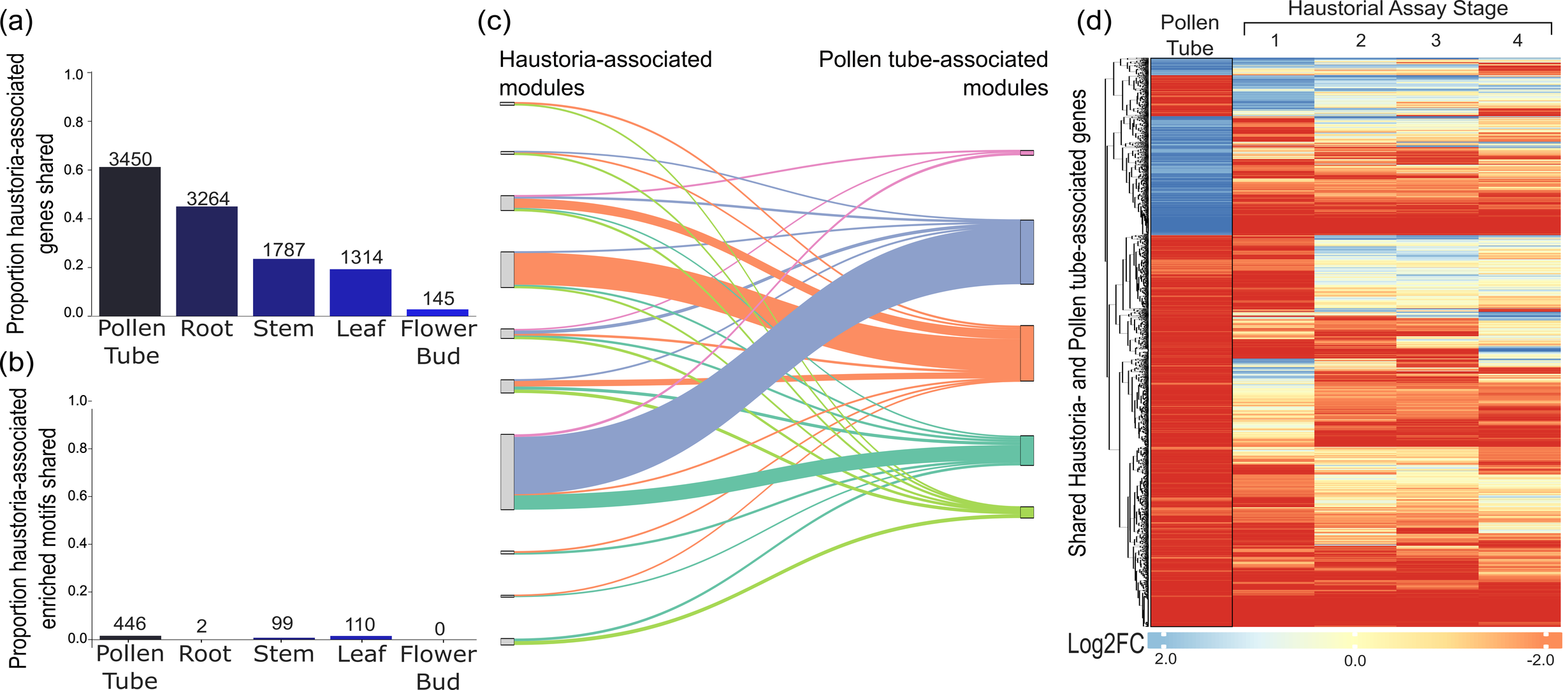
(a)
Proportion haustoria-associated genes shared
1.0
0.8
0.6
0.4
0.2
0.0
3450
3264
1787
1314
145
Pollen Tube
Root
Stem
Leaf
Flower Bud
(b)
Proportion haustoria-associated enriched motifs shared
1.0
0.8
0.6
0.4
0.2
0.0
446
2
99
110
0
Pollen Tube
Root
Stem
Leaf
Flower Bud
(c)
Haustoria-associated modules
Pollen tube-associated modules
(d)
Pollen Tube
Haustorial Assay Stage
1
2
3
4
Shared Haustoria- and Pollen tube-associated genes
Log2FC
2.0
0.0
-2.0

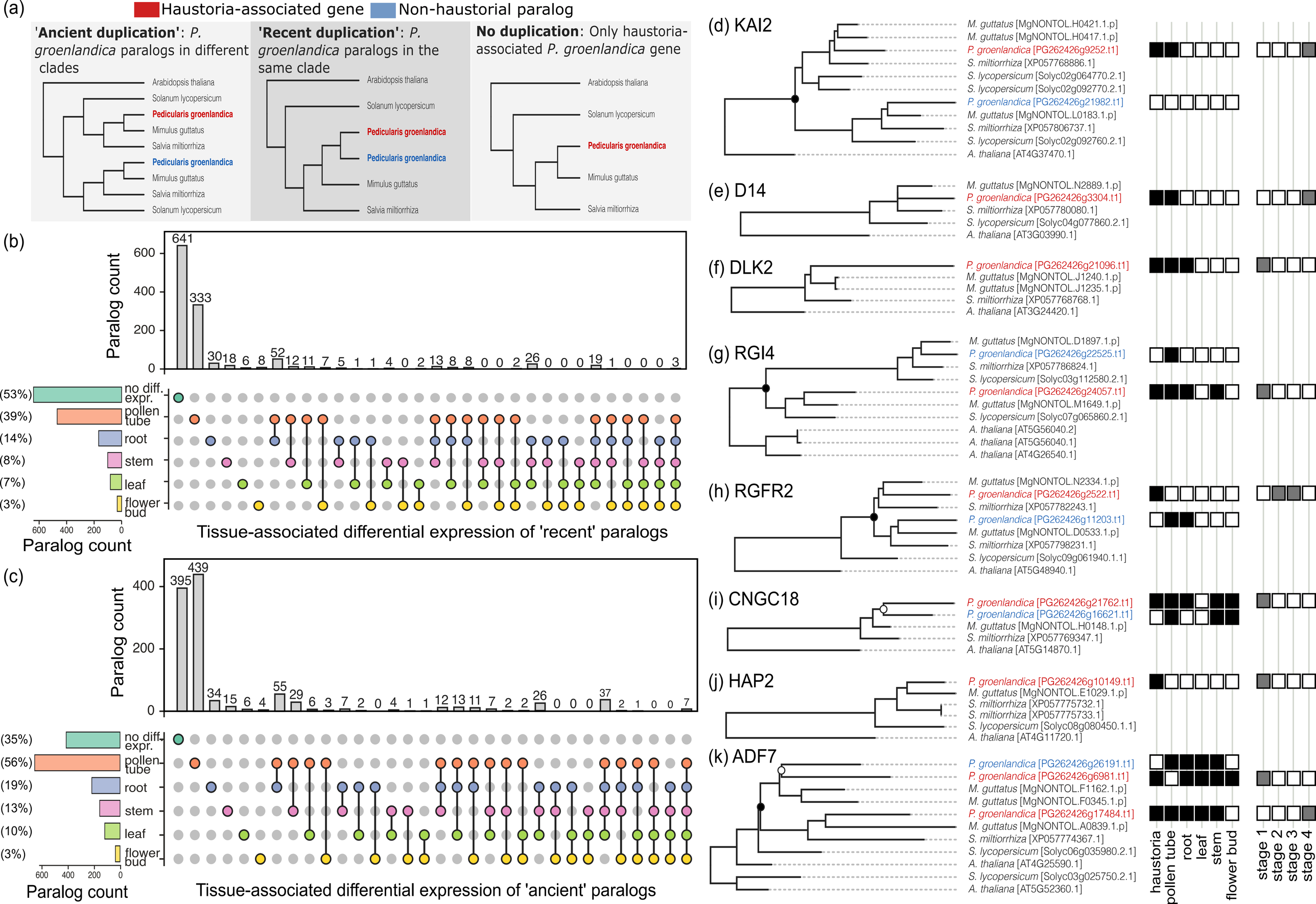
(a)
Haustoria-associated gene
Non-haustorial paralog
'Ancient duplication': P. groenlandica paralogs in different clades
'Recent duplication': P. groenlandica paralogs in the same clade
No duplication: Only haustoria-associated P. groenlandica gene
Arabidopsis thaliana
Solanum lycopersicum
Pedicularis groenlandica
Mimulus guttatus
Salvia miltiorrhiza
(b)
Paralog count
641
333
30 18 6 8 52 12 11 7 5 1 1 4 0 2 13 8 8 0 0 2 26 0 0 0 19 1 0 0 0 3
(53%) no diff. expr.
(39%) pollen tube
(14%) root
(8%) stem
(7%) leaf
(3%) flower bud
Tissue-associated differential expression of 'recent' paralogs
(c)
395 439
34 15 6 4 55 29 6 3 7 2 0 4 1 1 12 13 11 7 2 2 26 0 0 0 37 2 1 0 0 7
(35%) no diff. expr.
(56%) pollen tube
(19%) root
(13%) stem
(10%) leaf
(3%) flower bud
Tissue-associated differential expression of 'ancient' paralogs
(d) KAI2
M. guttatus [MgNONTOL.H0421.1.p]
M. guttatus [MgNONTOL.H0417.1.p]
P. groenlandica [PG262426g9252.t1]
S. miltiorrhiza [XP057768886.1]
S. lycopersicum [Solyc02g064770.2.1]
S. lycopersicum [Solyc02g092770.2.1]
P. groenlandica [PG262426g21982.t1]
M. guttatus [MgNONTOL.L0183.1.p]
S. miltiorrhiza [XP057806737.1]
S. lycopersicum [Solyc02g092760.2.1]
A. thaliana [AT4G37470.1]
(e) D14
M. guttatus [MgNONTOL.N2889.1.p]
P. groenlandica [PG262426g3304.t1]
S. miltiorrhiza [XP057780080.1]
S. lycopersicum [Solyc04g077860.2.1]
A. thaliana [AT3G03990.1]
(f) DLK2
P. groenlandica [PG262426g21096.t1]
M. guttatus [MgNONTOL.J1240.1.p]
M. guttatus [MgNONTOL.J1235.1.p]
S. miltiorrhiza [XP057768768.1]
A. thaliana [AT3G24420.1]
(g) RGI4
M. guttatus [MgNONTOL.D1897.1.p]
P. groenlandica [PG262426g22525.t1]
S. miltiorrhiza [XP057786824.1]
S. lycopersicum [Solyc03g112580.2.1]
P. groenlandica [PG262426g24057.t1]
M. guttatus [MgNONTOL.M1649.1.p]
S. lycopersicum [Solyc07g065860.2.1]
A. thaliana [AT5G56040.2]
A. thaliana [AT5G56040.1]
A. thaliana [AT4G26540.1]
(h) RGFR2
M. guttatus [MgNONTOL.N2334.1.p]
P. groenlandica [PG262426g2522.t1]
S. miltiorrhiza [XP057782243.1]
P. groenlandica [PG262426g11203.t1]
M. guttatus [MgNONTOL.D0533.1.p]
S. miltiorrhiza [XP057798231.1]
S. lycopersicum [Solyc09g061940.1.1]
A. thaliana [AT5G48940.1]
(i) CNGC18
P. groenlandica [PG262426g21762.t1]
P. groenlandica [PG262426g16621.t1]
M. guttatus [MgNONTOL.H0148.1.p]
S. miltiorrhiza [XP057769347.1]
A. thaliana [AT5G14870.1]
(j) HAP2
P. groenlandica [PG262426g10149.t1]
M. guttatus [MgNONTOL.E1029.1.p]
S. miltiorrhiza [XP057775732.1]
S. miltiorrhiza [XP057775733.1]
S. lycopersicum [Solyc08g080450.1.1]
A. thaliana [AT4G11720.1]
(k) ADF7
P. groenlandica [PG262426g26191.t1]
P. groenlandica [PG262426g6981.t1]
M. guttatus [MgNONTOL.F1162.1.p]
M. guttatus [MgNONTOL.F0345.1.p]
P. groenlandica [PG262426g17484.t1]
M. guttatus [MgNONTOL.A0839.1.p]
S. miltiorrhiza [XP057774367.1]
S. lycopersicum [Solyc06g035980.2.1]
A. thaliana [AT4G25590.1]
S. lycopersicum [Solyc03g025750.2.1]
A. thaliana [AT5G52360.1]
haustoria
pollen tube
root
leaf
stem
flower bud
stage 1
stage 2
stage 3
stage 4

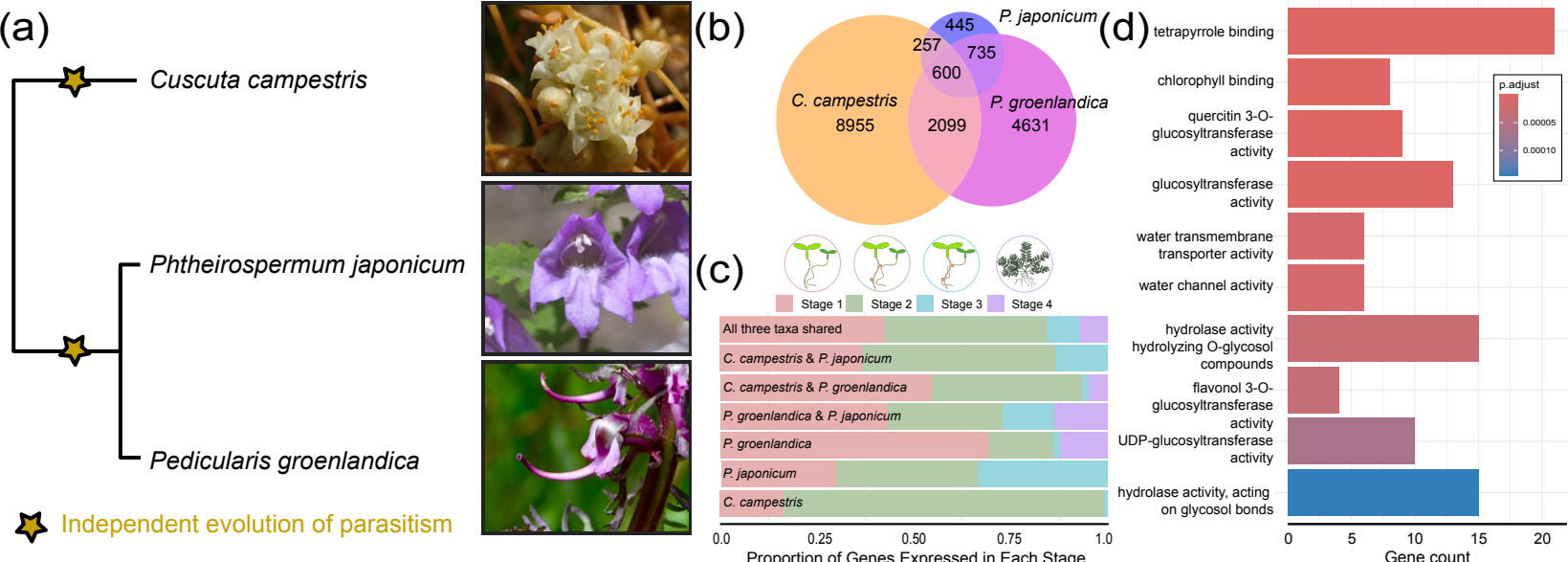
(a)
Cuscuta campestris
Phtheirospermum japonicum
Pedicularis groenlandica
Independent evolution of parasitism
(b)
P. japonicum
445
257
735
600
C. campestris
8955
2099
P. groenlandica
4631
(c)
Stage 1
Stage 2
Stage 3
Stage 4
All three taxa shared
C. campestris & P. japonicum
C. campestris & P. groenlandica
P. groenlandica & P. japonicum
P. groenlandica
P. japonicum
C. campestris
0.0
0.25
0.50
0.75
1.0
Proportion of Genes Expressed in Each Stage
(d)
tetrapyrrole binding
chlorophyll binding
quercitin 3-O-glucosyltransferase activity
glucosyltransferase activity
water transmembrane transporter activity
water channel activity
hydrolase activity hydrolyzing O-glycosol compounds
flavonol 3-O-glucosyltransferase activity
UDP-glucosyltransferase activity
hydrolase activity, acting on glycosol bonds
p.adjust
0.00005
0.00010
0
5
10
15
20
Gene count

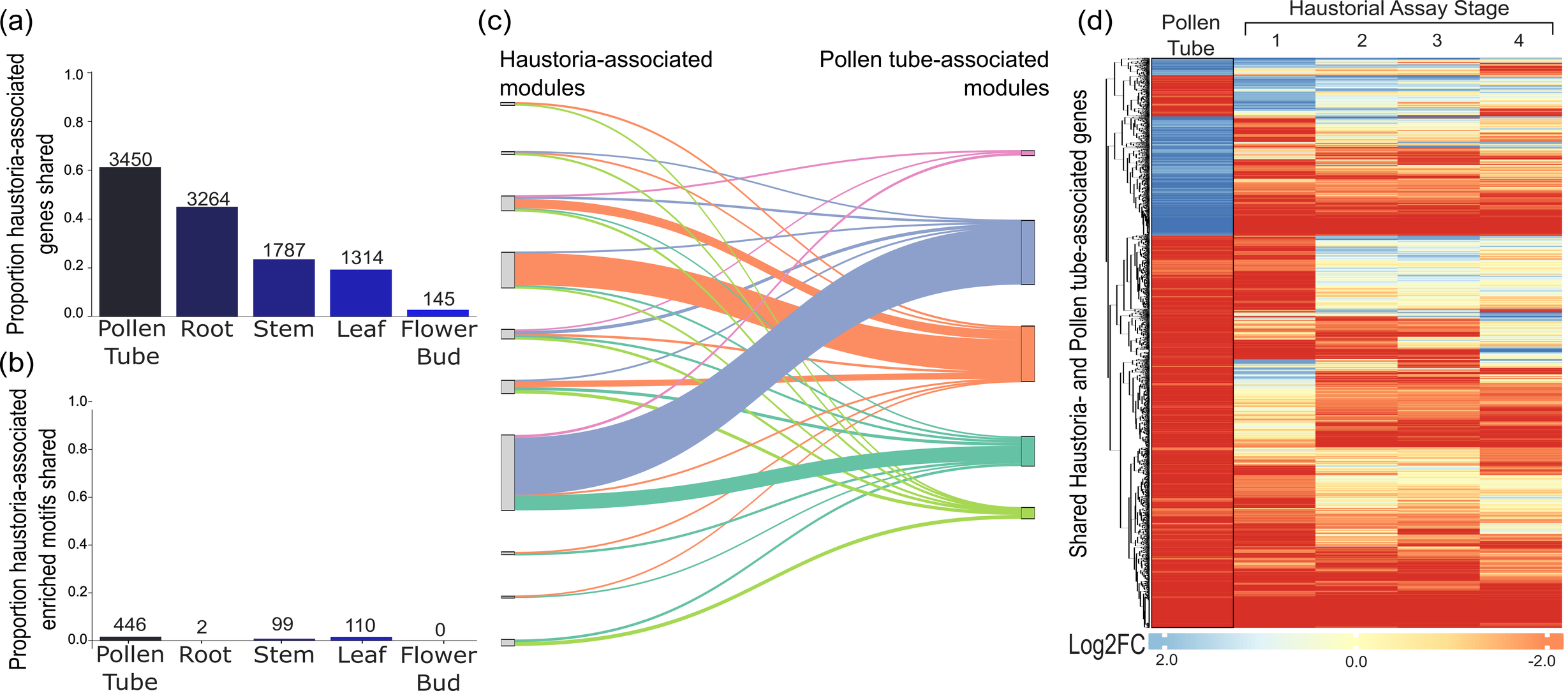
(a)
Proportion haustoria-associated genes shared
1.0
0.8
0.6
0.4
0.2
0.0
3450
3264
1787
1314
145
Pollen Tube
Root
Stem
Leaf
Flower Bud
(b)
Proportion haustoria-associated enriched motifs shared
1.0
0.8
0.6
0.4
0.2
0.0
446
2
99
110
0
Pollen Tube
Root
Stem
Leaf
Flower Bud
(c)
Haustoria-associated modules
Pollen tube-associated modules
(d)
Pollen Tube
Haustorial Assay Stage
1
2
3
4
Shared Haustoria- and Pollen tube-associated genes
Log2FC
2.0
0.0
-2.0

(a)

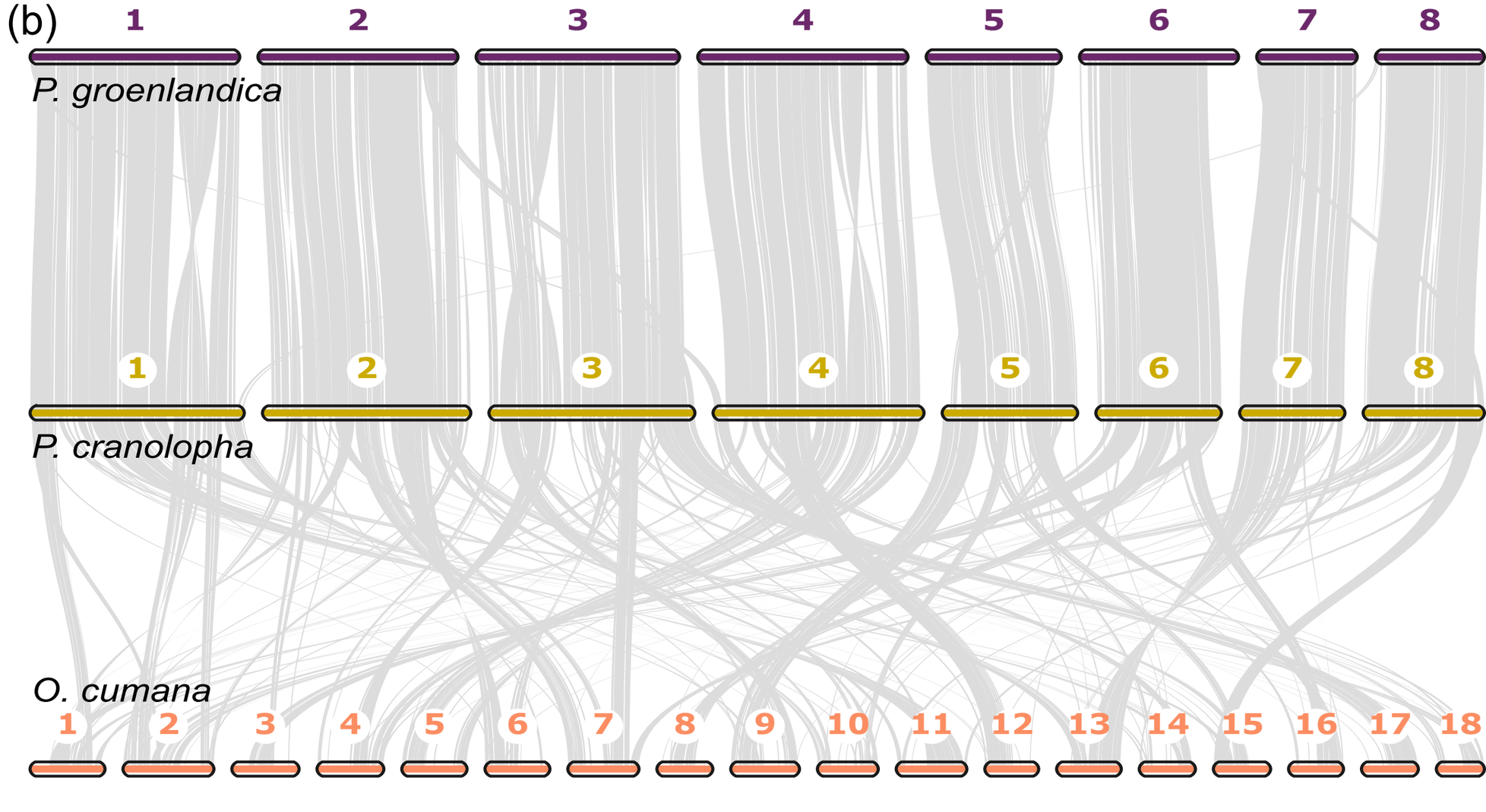
(b)
1
2
3
4
5
6
7
8
P. groenlandica
1
2
3
4
5
6
7
8
P. cranolopha
O. cumana
1
2
3
4
5
6
7
8
9
10
11
12
13
14
15
16
17
18

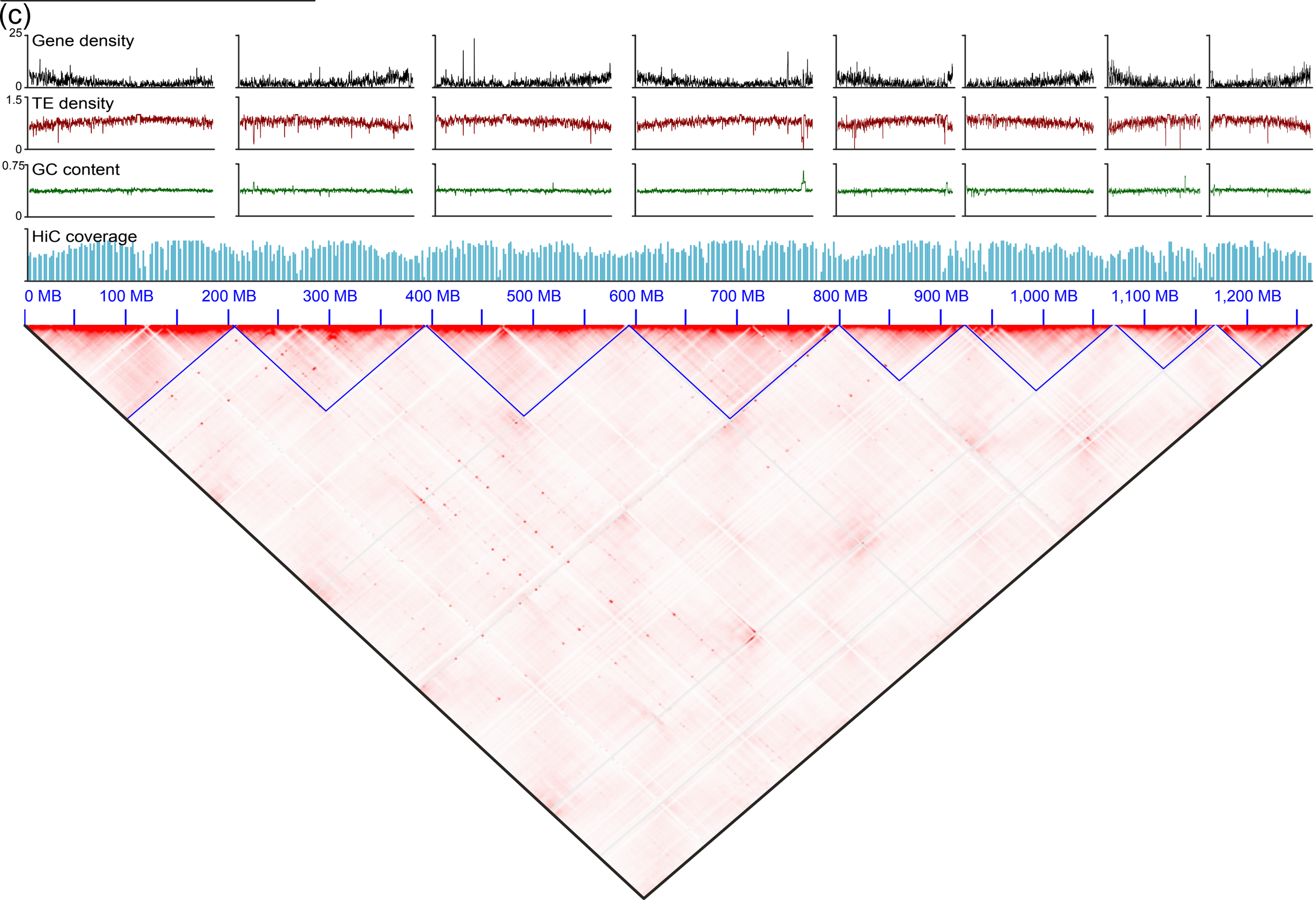
(c)
25
Gene density
0
1.5
TE density
0
0.75
GC content
0
HiC coverage
0 MB
100 MB
200 MB
300 MB
400 MB
500 MB
600 MB
700 MB
800 MB
900 MB
1,000 MB
1,100 MB
1,200 MB

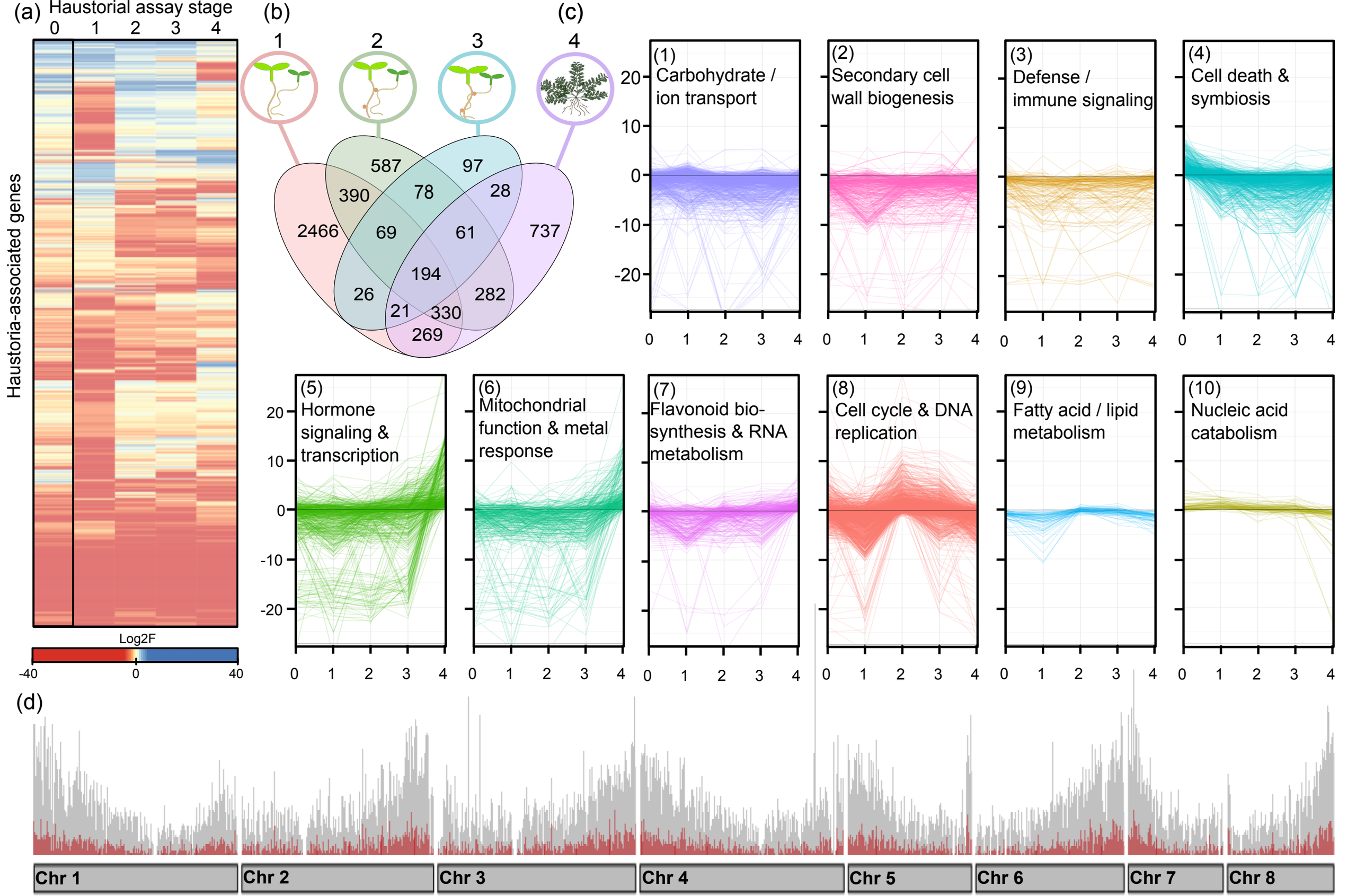
(a)
Haustorial assay stage
0 1 2 3 4
Haustoria-associated genes
Log2F
-40 0 40
(b)
1 2 3 4
587
97
390
78
28
2466
69
61
737
194
26
282
21
330
269
(c)
(1) Carbohydrate / ion transport
(2) Secondary cell wall biogenesis
(3) Defense / immune signaling
(4) Cell death & symbiosis
(5) Hormone signaling & transcription
(6) Mitochondrial function & metal response
(7) Flavonoid bio-synthesis & RNA metabolism
(8) Cell cycle & DNA replication
(9) Fatty acid / lipid metabolism
(10) Nucleic acid catabolism
20 10 0 -10 -20
0 1 2 3 4
(d)
Chr 1
Chr 2
Chr 3
Chr 4
Chr 5
Chr 6
Chr 7
Chr 8

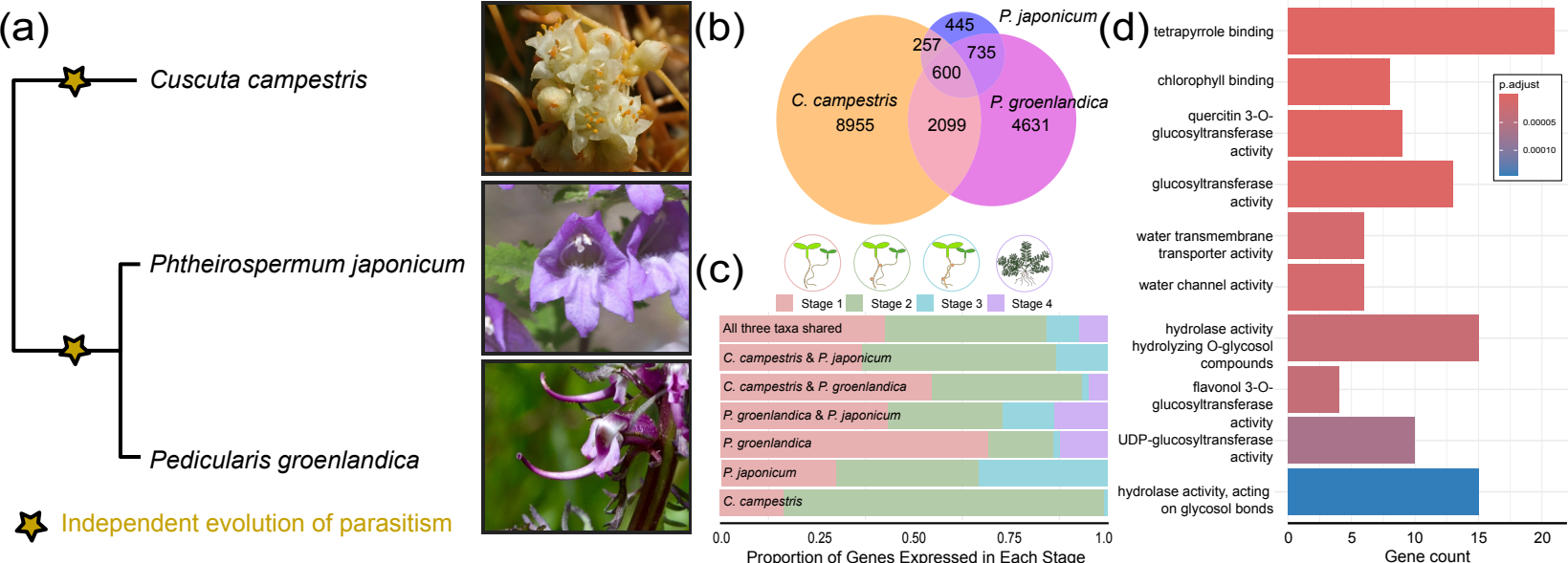
(a)
Cuscuta campestris
Phtheirospermum japonicum
Pedicularis groenlandica
Independent evolution of parasitism
(b)
P. japonicum
445
257
735
600
C. campestris
8955
2099
P. groenlandica
4631
(c)
Stage 1
Stage 2
Stage 3
Stage 4
All three taxa shared
C. campestris & P. japonicum
C. campestris & P. groenlandica
P. groenlandica & P. japonicum
P. groenlandica
P. japonicum
C. campestris
0.0
0.25
0.50
0.75
1.0
Proportion of Genes Expressed in Each Stage
(d)
tetrapyrrole binding
chlorophyll binding
quercitin 3-O-glucosyltransferase activity
glucosyltransferase activity
water transmembrane transporter activity
water channel activity
hydrolase activity hydrolyzing O-glycosol compounds
flavonol 3-O-glucosyltransferase activity
UDP-glucosyltransferase activity
hydrolase activity, acting on glycosol bonds
p.adjust
0.00005
0.00010
0
5
10
15
20
Gene count

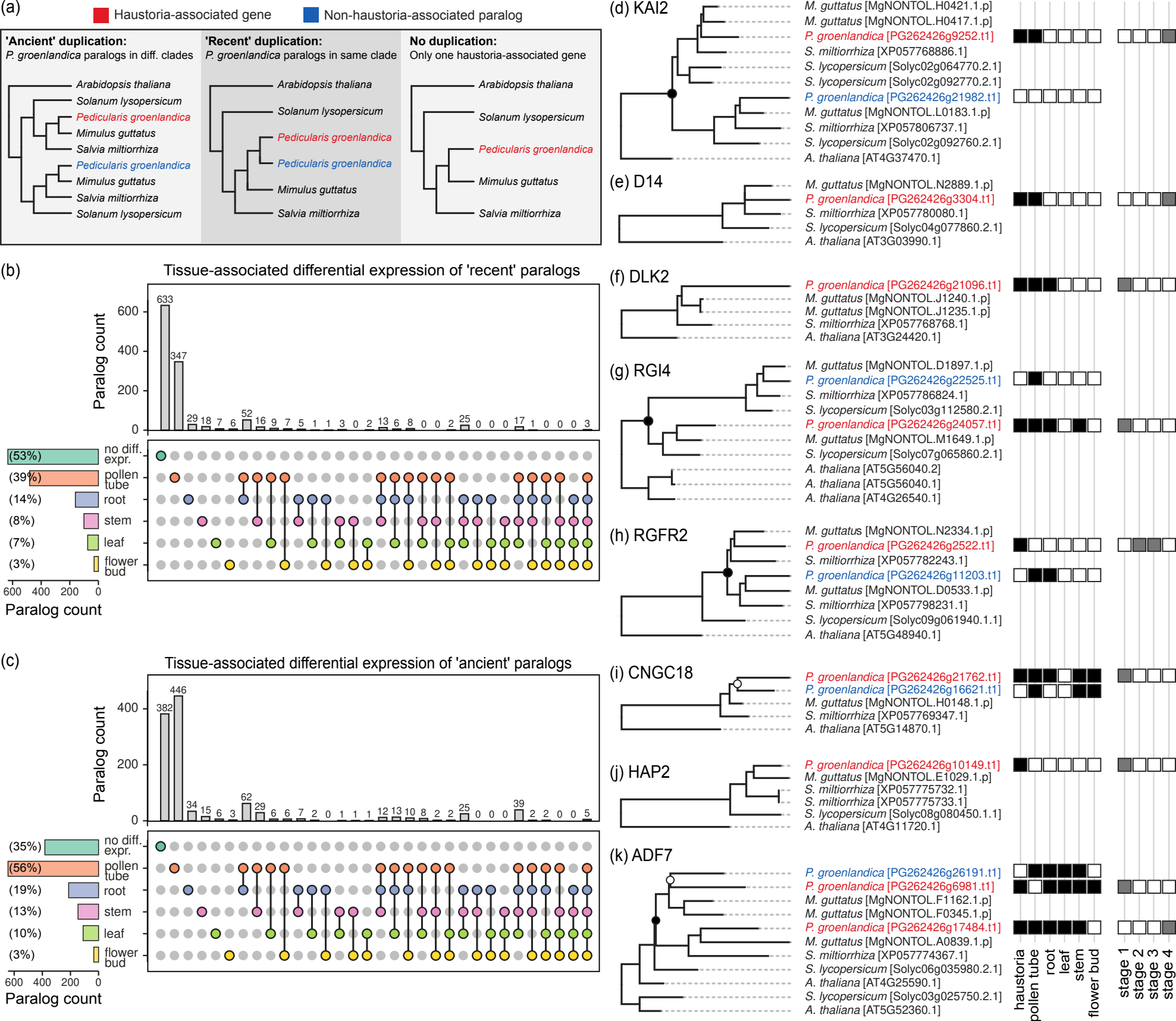
(a)
Haustoria-associated gene
Non-haustoria-associated paralog
'Ancient' duplication:
P. groenlandica paralogs in diff. clades
'Recent' duplication:
P. groenlandica paralogs in same clade
No duplication:
Only one haustoria-associated gene
Arabidopsis thaliana
Solanum lysopersicum
Pedicularis groenlandica
Mimulus guttatus
Salvia miltiorrhiza
(b)
Tissue-associated differential expression of 'recent' paralogs
Paralog count
no diff. expr.
pollen tube
root
stem
leaf
flower bud
(c)
Tissue-associated differential expression of 'ancient' paralogs
(d) KAI2
(e) D14
(f) DLK2
(g) RGI4
(h) RGFR2
(i) CNGC18
(j) HAP2
(k) ADF7
haustoria
pollen tube
root
leaf
stem
flower bud
stage 1
stage 2
stage 3
stage 4